eng

MDPI

Article

From Motor Efficiency to Loss Localization: A Phased, Field-Measurable Methodology for Evaluating Significant Energy Uses in Feed Mills

Yoisdel Castillo Alvarez [1,*], Reinier Jiménez Borges [2], José Pedro Monteagudo Yanes [3], Perla Yazmín Sevilla-Camacho [4,5], José Billerman Robles-Ocampo [4,5,*], Luis Angel Iturralde Carrera [6] and Juvenal Rodríguez-Reséndiz [6]

1 Department of Mechanical Engineering, Universidad Tecnológica del Perú (UTP), Lima 15046, Peru
2 Department of Mechanical Engineering, Faculty of Engineering, University of Cienfuegos "Carlos Rafael Rodríguez", Cienfuegos 59430, Cuba; rjimenezborges@gmail.com
3 Center for Energy and Environment Studies (CEEMA), Faculty of Engineering, University of Cienfuegos "Carlos Rafael Rodríguez", Cienfuegos 59430, Cuba; jpmyanes@ucf.edu.cu
4 Academic Group of Energy and Sustainability, Polytechnic University of Chiapas, Carretera Tuxtla Gutiérrez-Portillo Zaragoza Km 21+500, Col. Las Brisas, Suchiapa 29150, Mexico; psevilla@upchiapas.edu.mx
5 Division of Innovation in Advanced Technologies, Polytechnic University of Chiapas, Carretera Tuxtla Gutiérrez-Portillo Zaragoza Km 21+500, Col. Las Brisas, Suchiapa 29150, Mexico
6 Facultad de Ingeniería, Universidad Autónoma de Querétaro, Santiago de Querétaro 76010, Mexico; juvenal@uaq.edu.mx (J.R.-R.)
* Correspondence: c19773@utp.edu.pe (Y.C.A.); jrobles@upchiapas.edu.mx (J.B.R.-O.)

Abstract

In the feed industry, energy efficiency is typically assessed using aggregate consumption indicators (kWh/t) or the efficiency of the electric motor in isolation, which makes it impossible to pinpoint where energy is lost along the conversion chain. This study formalizes a three-phase methodology that breaks down the useful electrical efficiency of each Significant Energy Use (SEU) into its successive stages—motor, transmission, and process—based on field-measurable variables, linking electrical conversion with the useful power model of each machine. The process efficiency of hammer mills is normalized using the Swiss Institute of Feed Technology (SFT) reference index; this constitutes a load-sensitive performance ratio, not an absolute thermodynamic efficiency. Its demonstration at the "Piensos Cienfuegos" plant (Cuba), using data from a 2015 industrial campaign, yielded overall efficiencies of 72% for the bucket elevator—conditional on the adopted nominal throughput and nameplate power factor, with a plausible range of 43–89% under coupled systematic-bias scenarios—26–28% for the hammer mills—despite motors operating at 90–92% efficiency—and 17.3% for the screw conveyor (24.7% at the processing stage). Grinding efficiency fell from 31.1% to 9.7% as the throughput of Mill III was reduced from 16 to 5 t/h, corresponding to an increase in normalized shaft-specific energy consumption from 3.50 to 11.2 kWh/t. The expanded measurement uncertainty was 11.8% ($k = 2$), and systematic sources of uncertainty were quantified through a sensitivity analysis. The scope of this work is diagnostic: no retrofit or operational intervention was implemented at the plant, and consequently no before–after energy savings are measured or claimed. The reported efficiencies characterize the baseline condition and identify where intervention would be effective.

Keywords: energy efficiency; feed industry; hammer mill; bucket elevator; screw conveyor; loss decomposition; partial-load operation; significant energy uses (SEUs); ISO 50001; ISO 50015; measurement and verification; energy management

Check for updates

Academic Editor: Antonio Gil Bravo

Received: 23 July 2026
Revised: 13 August 2026
Accepted: 17 August 2026
Published: 25 August 2026

Copyright: © 2026 by the authors. Licensee MDPI, Basel, Switzerland. This article is an open access article distributed under the terms and conditions of the Creative Commons Attribution (CC BY) license.

1. Introduction

The compound feed industry is one of the most energy-intensive sectors within the agri-food supply chain. Feed accounts for approximately 70% of livestock production costs [1], and, within feed manufacturing plants, size reduction is the unit operation with the highest electricity demand [2,3]. Grinding increases the specific surface area of feed ingredients, enhances nutrient availability, and improves animal performance [4–6], making it an indispensable operation in the production of swine and poultry feeds [7,8]. This nutritional benefit comes at an energy cost: hammer mills can account for up to half of the total electricity demand of a feed mill [9]. Consequently, improving their operating efficiency provides a direct pathway to reducing electricity consumption without compromising production.

The energy demand of grinding is governed by the principles of comminution discussed in Section 2.7. Building on this foundation, numerous studies have investigated the specific energy consumption of hammer mills as a function of rotor speed, screen size, moisture content, and the physical properties of the processed material [10–13]. The resulting particle size distributions and the mathematical models developed to predict them have also received sustained attention [14–18]. Other authors have compared hammer and roller mills in terms of specific energy consumption, particle size distribution, and grain and feed quality [19–21], while the effects of hammer geometry, screen configuration, and feedstock moisture content have been examined in detail [22–25]. Downstream of the grinding stage, conditioning and pelleting also require substantial amounts of energy and strongly influence the quality of the final product [26–28]. Recent coupled numerical–experimental work has extended the grinding literature toward CFD–DEM analysis, quantifying the influence of spindle speed, hammer–screen gap, and screen aperture on grinding performance and energy dissipation [29].

The internal handling of bulk solids constitutes the second largest source of electricity consumption in the feed industry. Among the available conveying alternatives, screw conveyors are widely used for dosing and transporting particulate solids. Their performance has traditionally been described through empirical correlations, although recent studies have incorporated the Discrete Element Method (DEM) to evaluate mass flow rate, power requirements, and energy dissipation mechanisms [30–32], and current reviews of granular flow in screw conveyors consolidate the influence of rotational speed, inclination angle, and fill level on transport efficiency and power demand [33]. The optimization of these systems from an energy-efficiency perspective [34–36], together with the consistency achieved between analytical models, numerical simulations, and experimental results [37], and the more recent use of data-driven estimators of conveyed mass flow rate [38], has further strengthened this body of knowledge. Bucket elevators, by contrast, provide vertical conveying with comparatively low energy losses, as most of the supplied energy is expended in overcoming gravity.

Electric motors provide the mechanical power required by all these operations, and their efficiency, together with their operating load, largely determines the overall electricity consumption of the plant. The adoption of high-efficiency motors [39] and variable speed drives [40] is widely recognized as an effective strategy for improving the performance of motor-driven systems. From the perspective of energy management, ISO 50001 promotes the systematic evaluation and continual improvement of energy performance through the use of Energy Performance Indicators (EnPIs), which constitute the methodological foundation of the framework developed in this study. Industrial applications of ISO 50001 have consistently demonstrated measurable improvements in energy performance [41,42]. Recent manufacturing-level evidence likewise reports persistent energy-performance improvements under ISO 50001-based systems [43,44]. The evaluation

of that performance, however, requires an explicit measurement and verification (M&V) basis, which is established by ISO 50015 and, for process-level audits, by ISO 50002-3 [45,46]; this requirement is addressed in Section 2.3.

Despite the breadth of the available literature, an important methodological gap remains. Studies on grinding estimate the energy required for size reduction but rarely extend the analysis to the subsequent stages of the energy conversion chain. Research on bulk solids handling has established design power requirements and conveying efficiencies without integrating them into a comprehensive assessment of the complete electrical energy conversion process. Likewise, energy management studies primarily focus on plant-wide energy consumption and energy baseline development, placing less emphasis on the performance of individual equipment or on the distribution of losses across successive conversion stages. The recently validated mathematical model for hammer mills [9], which incorporates throughput, moisture content, absorbed power, and hammer wear beyond the assumptions of classical comminution equations, represents a significant step in this direction, although it is limited to a single equipment category. To the best of the authors' knowledge—a claim substantiated by the representative literature review presented in Section 4.1—no unified, reproducible, and practically applicable methodology has yet been reported that evaluates the energy efficiency of different categories of high-energy-consuming equipment under a common analytical framework while localizing losses throughout the entire electrical-to-useful energy conversion chain under real operating conditions. This work addresses that limitation by extending the energy assessment methodologies for agro-industrial and bioenergy systems previously developed by the authors [3,47].

To address this gap, a generalizable three-phase methodology is formalized. Phase 1 performs the energy characterization of the plant and identifies the Significant Energy Uses (SEUs) in accordance with ISO 50001. Phase 2 establishes a unified calculation procedure that determines the efficiency of each equipment category by decomposing it into its successive energy conversion stages—motor, transmission, and process—using electrical and process variables measurable in the field, together with the appropriate useful power model for each machine. For hammer mills, the Bond formulation normalized to the reference index of the Swiss Institute of Feed Technology (SFT) is adopted [9,48]; for the bucket elevator and screw conveyor, bulk solids-handling flow and power models are applied. Phase 3 implements the methodology under real operating conditions, synthesizes the resulting efficiencies by equipment type, and evaluates the associated measurement uncertainty. The novelty of the proposed approach lies in the formalization of a unified procedure applicable to physically heterogeneous equipment and in its reliance on field-measurable variables, making it transferable to any feed manufacturing plant and, more broadly, to industrial facilities requiring the diagnosis of the energy efficiency of their major energy-consuming equipment.

Accordingly, the overall objective of this study is to formulate and demonstrate a generalizable methodology, based on electrical and process variables measurable in the field, for determining the stage-wise energy efficiency of major energy-consuming equipment in the feed industry.

The methodology is demonstrated through its application at the "Piensos Cienfuegos" feed mill (Cuba), considering hammer mills, a screw conveyor, and a bucket elevator as the plant's SEUs, evaluated under three production levels (600, 360, and 100 t/day). It is important to emphasize that this work is conceived as a single-case demonstration rather than as a statistical or cross-sector validation. The primary contribution is the methodology itself—a unified procedure implementable through field measurements—while the industrial case study serves to demonstrate its applicability and practical feasibility. The study is

furthermore diagnostic in scope: no retrofit or operational intervention was carried out, and no before–after energy savings are claimed.

The remainder of the paper is organized as follows. Section 2 presents the case study and the proposed three-phase methodology. Section 3 applies the methodology to the selected industrial process, reporting the estimated equipment efficiencies, their dependence on production load, the distribution of losses along the energy conversion chain, and the associated uncertainty analysis. Section 4 compares these findings with previous studies and discusses the applicability and limitations of the proposed approach. Finally, Section 5 summarizes the main conclusions and outlines directions for future research.

2. Materials and Methods

2.1. General Methodological Framework

The proposed approach is based on the principle of loss localization for evaluating the energy performance of industrial plants. Determining the electricity consumption of each machine is a necessary starting point, but this information alone does not reveal how energy is dissipated throughout the successive conversion stages, from the electric motor to the useful process output. To overcome this limitation, a unified performance indicator is introduced that is applicable to equipment performing different physical functions: electrical-to-useful efficiency, defined as the product of the efficiencies associated with each conversion stage—electric motor, mechanical transmission, and industrial process. Under this formulation, hammer mills, screw conveyors, and bucket elevators can be analyzed within a common framework while preserving the ability to identify the dominant sources of energy loss in each system.

The methodology is structured into three consecutive phases. In Phase 1, the overall energy performance of the plant is evaluated in accordance with ISO 50001 [49,50], and the Significant Energy Uses (SEUs) are identified. In Phase 2, the electrical energy conversion model is integrated with the useful power model corresponding to each SEU, allowing the efficiencies of the successive conversion stages to be estimated from electrical and process variables measurable under real operating conditions. Phase 3 implements the methodology in industrial operating scenarios under different production loads, determining equipment efficiencies and quantifying losses at each conversion stage. This final phase makes it possible to distinguish between losses that are inherent to the process and those that can be mitigated through operational strategies or technological improvements.

The complete procedure is illustrated in Figure 1. Rather than proposing isolated new calculations, the principal contribution of this work lies in integrating established analytical approaches into a coherent framework that is practical, reproducible, auditable, and applicable to different categories of industrial equipment.

The logic underlying Figure 1 makes the decision structure of the proposed framework explicit. The two decision diamonds encode successive diagnostic questions: first, whether a given piece of equipment constitutes a Significant Energy Use (SEU) that warrants detailed analysis; and second, at which energy conversion stage its losses are predominantly concentrated. Consequently, the output of the procedure is not merely a scalar performance indicator but a classified management action: an operational intervention when process losses depend on the production load, an investment decision when the losses are intrinsic to the physical operating principle of the equipment, or no intervention when the equipment already operates close to its practical performance limit. This decision-oriented structure transforms loss decomposition into a practical energy management tool fully consistent with the principles of ISO 50001.

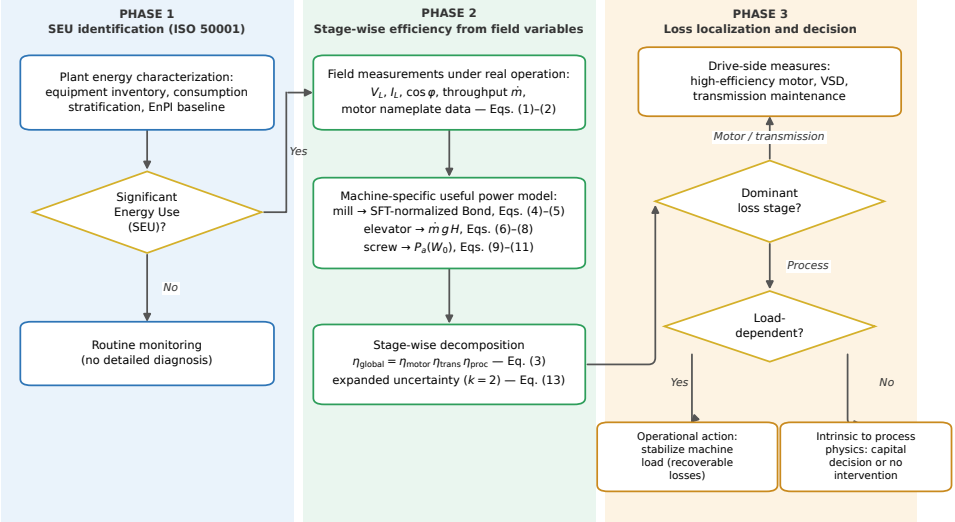

Figure 1. Decision flowchart of the proposed three-phase methodology. Diamonds represent decision points; the principal governing equations of the quantitative blocks are indicated within the diagram.

2.2. Plant Description and Energy Characterization

The proposed methodology was applied at the "Piensos Cienfuegos" feed manufacturing plant (Cuba). The facility is organized into five main production sections: raw material reception and storage, grinding, dosing and mixing, pelleting, and soybean and limestone reception. Since electricity is the predominant energy carrier throughout all operations, the analysis focuses on electrical energy efficiency at both the process and equipment levels. In accordance with ISO 50001 [49,50], and following the guidance on Energy Performance Indicators (EnPIs) and energy baselines provided by ISO 50006 and ISO 50004 [51,52], the plant's electricity consumption was disaggregated to identify the SEUs, a step widely recognized as fundamental for improving industrial energy performance [53–55].

The assessment of the equipment inventory—considering installed capacity, operating time, and electricity consumption—produced the consumption stratification shown in Figure 2, which follows the analysis sequence plant supply → production section → significant energy use. Grinding and pelleting together account for approximately 76% of the plant demand, and within the grinding section, the hammer mills and their associated material-handling systems concentrate about 90% of the sectional consumption. On this basis, the methodology was applied to the principal mechanical SEUs of the production line: the hammer mills, one bucket elevator, and one screw conveyor.

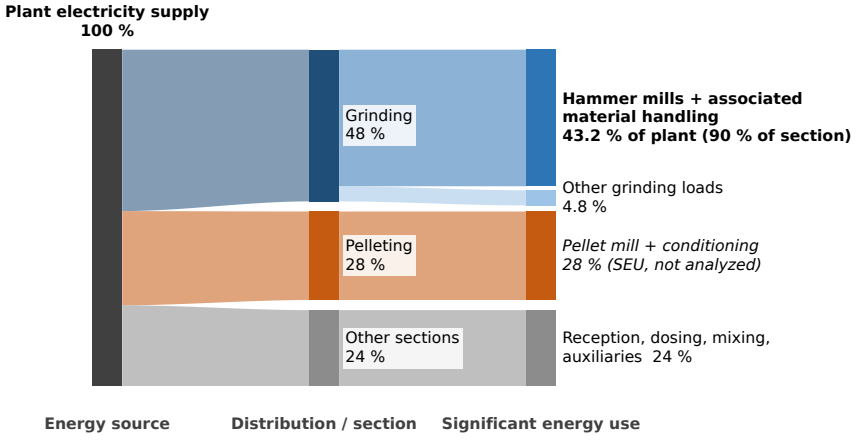

Figure 2. Stratification of the plant electricity consumption. Percentages refer to the total plant demand.

The pelleting process was not included in the present analysis because its thermomechanical behavior requires a different measurement approach and specialized instrumentation. The specific variables and instrumentation required to incorporate it into the same framework are specified in Section 4.4. During the industrial measurement campaign, the feed formulation consisted of approximately 68% corn and 32% soybean meal. Measurements were performed under three production rates—600, 360, and 100 t/day—corresponding to high-, medium-, and low-load operating conditions, respectively.

2.3. Data Sources, Instrumentation, and Measurement Protocol

The operational and geometric data used in this study originate from an industrial measurement campaign conducted in 2015 at the "Piensos Cienfuegos" plant and documented in an undergraduate engineering thesis at the University of Cienfuegos. The campaign provided the production records, daily electricity consumption data, motor nameplate specifications, operating currents, screw conveyor geometry, and the dimensions and operating parameters of the bucket elevator. In contrast, the calculation procedure, the stage-wise efficiency decomposition, the loss allocation methodology, the uncertainty analysis, and the treatment of load effects presented in this work constitute a new methodological formulation. They neither reproduce the results of the original campaign nor reuse its calculation procedure, whose structural limitations are discussed in Section 2.7.1. This distinction—legacy data, new methodology—is essential for correctly interpreting the scope and contribution of the present case study.

During the measurement campaign, the line voltage (V_L) and line current (I_L) of each equipment unit were recorded under normal operating conditions. The original documentation does not report the instrument models, measurement accuracy, calibration status, or sampling frequency. This limitation is explicitly acknowledged and incorporated into the uncertainty budget through the assumed instrument accuracies described in Section 3.5. The power factor ($\cos \varphi$) and motor efficiency were obtained from the motor nameplate specifications and standardized efficiency classes [56,57]. Since both parameters may deviate from their nominal values under partial-load operation, they were treated as systematic sources of uncertainty through sensitivity analysis.

The throughput values used in this study have three distinct levels of traceability, which are explicitly identified to preserve the metrological transparency of the assessment. (i) The hammer mill throughputs under the 600 t/day operating condition (16–17 t/h) were obtained from the plant production records and are consistent with the documented daily production and operating hours. (ii) The 5 t/h throughput of Hammer Mill III, corresponding to the soybean processing campaign at 360 t/day, originates from the legacy records collected in 2015. The associated documentation contains internal inconsistencies between daily production, operating hours, and instantaneous throughput; consequently, this value is treated as legacy data with documentary uncertainty, whose implications are discussed in Section 3.3 and the limitations section. (iii) The throughputs of the screw conveyor and bucket elevator correspond to their nominal operating values, which are consistent with the geometric parameters through Equations (6) and (9), since no in-line gravimetric measurements were available for the bulk solids-handling systems. This distinction is important because throughput constitutes the dominant contributor to the uncertainty budget of the proposed methodology (Section 3.5).

Simultaneously, the relevant process variables (particle size distribution, where applicable, together with the geometric and filling parameters of each machine) and the motor nameplate data (rated power, rated power factor, rotational speed, and nominal efficiency) were recorded. Prior to the measurement campaign, the plant lacked the information required to quantify the operating efficiency of its major energy-consuming

equipment. The systematic data acquisition carried out in this study therefore provides the measurements necessary for evaluating and monitoring the plant's energy performance.

Measurement and Verification Plan

The evaluation of energy performance requires an explicit measurement and verification (M&V) basis; otherwise, statistical propagation is used to compensate for a measurement protocol that was never declared. The measurement plan associated with the proposed framework is therefore specified here in accordance with the general principles of ISO 50015 [45], complemented by the guidance for process-level energy audits of ISO 50002-3 [46] and by the EnPI and energy baseline provisions of ISO 50006 [51]. Six elements are declared.

(i) Boundary: each SEU is treated as an individual measurement boundary, with the electrical supply at the motor terminals as the input port and the equipment-specific useful power model as the output port. (ii) Relevant variables: line voltage, line current, power factor, and processed mass flow rate. (iii) Static factors: material type, screen aperture, and equipment configuration, held constant within each operating condition. (iv) Measurement method: for a compliant campaign, three-phase power loggers with energy integration over a period covering at least one full production cycle, at a sampling interval no coarser than 1 min, together with in-line gravimetric flow measurement; spot readings of line current combined with an assumed nameplate power factor—the method available in the legacy 2015 campaign—do not satisfy this requirement. Where the supply serves an aged motor population, the plan should additionally record voltage unbalance and total harmonic distortion, since both degrade the actual motor efficiency relative to its nameplate class and would otherwise be absorbed into the transmission-stage balance-closure term (Section 2.7). (v)Uncertainty: quantified in Section 3.5 for the random component and bounded by scenario analysis for the systematic component. (vi) Reporting period: not applicable in the present study, since no intervention was implemented.

This declaration serves two purposes. It specifies the measurement protocol required for a compliant application of the proposed framework, and it makes explicit the gap between that protocol and the legacy dataset used in this demonstration, so that the two are not confused. The framework is defined at the level (iv) protocol; the case study operates below it, and the consequences of that gap are carried through the uncertainty analysis and the limitations section.

2.4. Equipment Characteristics and Operating Data

The equipment analyzed in this study was characterized using three complementary sets of information: motor nameplate specifications, the geometric and operating parameters of the material-handling equipment, and the electrical and process measurements collected during plant operation. All measurements were performed at the supply voltage (440 V) under normal industrial operating conditions. Table 1 summarizes the motor nameplate specifications together with the operating current ratio.

The installed motors exhibit relatively high nominal efficiencies, ranging from 82.5 to 92%. The current ratio $k_I = I_L / I_{\text{nom}}$ is used as an indicator of the operating regime of each unit: values below 100% indicate operation below the rated current. It should be emphasized, however, that k_I does not represent the true mechanical load factor of the motor. Under reduced load conditions, the magnetizing component of the current—which is approximately independent of the load—causes k_I to overestimate the fraction of useful power demand, with this bias increasing as the load decreases. A conversion into a true load factor would require the motor characteristic curve, direct shaft power measurements, or slip estimation, none of which were available from the measurement campaign. With this

limitation in mind, all units operated below their rated current: the bucket elevator exhibited the lowest current ratio (42%), followed by Hammer Mill III (47%), the screw conveyor (60%), and Hammer Mills II and IV (74%). The influence of these operating conditions on the overall performance is examined in Section 3.

Table 1. Motor nameplate specifications and operating current ratio, $k_I = I_L / I_{\text{nom}}$, of the major energy-consuming equipment.

Equipment	P_{nom} (kW)	$\cos\varphi$	n (rpm)	η_{motor} (%)	k_I (%)
Hammer Mill II	132	0.86	1192	91.0	74
Hammer Mill III	132	0.86	1192	90.0	47
Hammer Mill IV	132	0.86	1192	92.0	74
Screw Conveyor	3.60	0.86	1750	82.5	60
Bucket Elevator	11.0	0.86	1172	87.0	42

For the hammer mills, I_{nom} was obtained as $P_{\text{nom}}/(\sqrt{3}\,V_L \cos\varphi)$; for the screw conveyor and the bucket elevator, the rated current declared on the motor nameplate was used directly.

The geometric and operating parameters required by the useful power models for bulk solids handling are listed in Table 2. These parameters define the operating conditions of the screw conveyor and bucket elevator and provide the input data for the calculations presented in the following sections.

Table 2. Geometric and operating parameters of the bulk solids-handling equipment used in the useful power models (Equations (6)–(10)).

Parameter	Screw Conveyor	Bucket Elevator
Length L/lifting height H (m)	1.70	46.10
Diameter D (m)	0.40	—
Screw pitch p (m)	0.32	—
Inclination angle β (°)	5	—
Rotational speed n (rpm)	79	—
Section filling coefficient ψ	0.32	—
Inclination coefficient K	0.90	—
Total resistance coefficient W_0	1.60	—
Bucket volume i (L)	—	6.3
Bucket height h (mm)	—	210
Bucket spacing t (m)	—	0.42
Bucket filling coefficient j	—	0.70
Mass per bucket $M = i\rho j$ (kg)	—	3.62
Belt velocity v (m/s)	—	1.10
Equivalent loading height H_0 (m)	—	3.8
Nominal throughput Q (t/h)	45	34
Bulk density ρ (kg m^{-3})	820	820

The parameters listed in Table 2 are consistent with the properties of the transported material. The filling coefficient $\psi = 0.32$ and the total resistance coefficient $W_0 = 1.6$ correspond to lightweight, low-abrasiveness bulk materials, such as cereal grains, according to the classical classification of bulk solids-handling systems [58]. The equivalent loading height $H_0 = 3.8$ m represents the resistance associated with bucket filling and is accounted for in the adopted model as a transmission loss rather than as useful lifting work.

Table 3 summarizes the measured electrical variables and operating throughputs of each equipment unit, which constitute the input data for the models described in Section 2.7.

The measurements reveal marked differences in electrical demand among the analyzed equipment. Under the evaluated operating conditions, the three hammer mills required a combined electrical power of 258.6 kW, whereas the screw conveyor and bucket elevator consumed a combined 7.9 kW. The measured currents of all units remained below their

rated values, in agreement with the current ratios reported in Table 1. These results provide the basis for the efficiency calculations and the analysis presented in Section 3.

Table 3. Measured electrical variables, calculated electrical power (Equation (1), $\sqrt{3} \approx 1.73$), throughput, and processed material at the 600 t/day production level. $V_L = 440$ V.

Equipment	V_L (V)	I_L (A)	P_{elect} (kW)	Throughput (t/h)	Material
Hammer Mill IV	440	150	98.19	17.0	Corn
Hammer Mill II	440	150	98.19	17.0	Corn
Hammer Mill III	440	95	62.19	16.0	Soybean
Screw Conveyor	440	3.1	2.03	45 †	—
Bucket Elevator	440	9.0	5.89	34 †	—

† The hammer mill throughputs under this operating condition (600 t/day) were obtained from the plant production records; the 5 t/h throughput of Hammer Mill III used in Section 3.3 corresponds to legacy data from the 2015 campaign with documentary uncertainty (Section 2.3). The screw conveyor and bucket elevator throughputs are nominal operating values—consistent with Equations (6) and (9) and the parameters reported in Table 2—rather than in-line gravimetric measurements.

2.5. Unified Framework: Operational Efficiency and Energy Conversion Chain

The efficiency of all equipment categories is determined using a common analytical basis. The electrical input power supplied to the motor is calculated from the measured line variables according to Equation (1):

$$P_{\text{elect}} = \sqrt{3}\, V_L\, I_L\, \cos\varphi, \tag{1}$$

whereas the motor efficiency (normalized according to the NEMA/IEC efficiency classes [56,57]) relates shaft power to electrical input power, as expressed in Equation (2):

$$\eta_{\text{motor}} = \frac{P_{\text{shaft}}}{P_{\text{elect}}} \implies P_{\text{shaft}} = \eta_{\text{motor}}\, P_{\text{elect}}. \tag{2}$$

The global efficiency of any equipment unit is expressed as the product of the efficiencies associated with its successive energy conversion stages, following the cascade decomposition commonly used for motor-driven systems [9,59]:

$$\eta_{\text{global}} = \frac{P_{\text{useful}}}{P_{\text{elect}}} = \eta_{\text{motor}} \cdot \eta_{\text{trans}} \cdot \eta_{\text{proc}}, \tag{3}$$

where η_{proc} is equipment-specific and represents the conversion of shaft power into useful process output. For hammer mills, it corresponds to the grinding efficiency normalized against the sector reference index (Section 2.7); for the screw conveyor, it represents the transport performance ratio, namely the fraction of the screw shaft power that corresponds to the theoretical conveying power requirement; and for the bucket elevator, it is assumed to be approximately unity, since lifting the material against gravity constitutes the useful work directly delivered by the transmission. It should be noted that Equation (3) has an important structural property from a metrological perspective: the global efficiency depends only on P_{useful} and P_{elect}, making it invariant to errors in the allocation between η_{motor} and η_{trans}. Therefore, biases in nameplate-derived values affect the attribution of losses among conversion stages but do not modify the global equipment diagnosis for a given throughput. This structure—a common electrical basis combined with an equipment-specific process efficiency—enables the evaluation and comparison of physically heterogeneous machines within a unified analytical framework.

2.6. Global Efficiency Under Real Operating Conditions

Since feed mills frequently operate below their rated capacity—a condition that increases the effects of motor oversizing and partial-load operation [60,61]—the efficiency of each equipment unit is evaluated under actual operating conditions. Whenever sufficient data are available, the analysis is repeated at different production levels to characterize the dependence of efficiency on operating load (Section 3). No empirical correction or adjustment factors are introduced; each efficiency value is calculated directly from the variables corresponding to the evaluated operating condition.

2.7. Useful Power Models by Equipment Category

Classical comminution and bulk solids-handling sources are cited in this section as the primary formulations of the governing equations, not as representative of the current state of the art, which is addressed in Section 4.1.

2.7.1. Hammer Mill: Efficiency Normalized to the SFT Reference

The useful grinding power is estimated using the Bond comminution framework [62] historically preceded by Rittinger's [63] and Kick's [64] laws and later incorporated into process engineering practice [65,66] normalized to the reference index of the Swiss Institute of Feed Technology (SFT) [48], following the methodological approach adopted in the validated model reported in [9]. The specific reference index for each material and screen configuration is obtained from the tabulated grinding factor JKM, as shown in Equation (4):

$$W_{i,\mathrm{ref}} = \frac{1000}{\phi\ JKM}, \tag{4}$$

where ϕ is the screen diameter (mm) and JKM is the cereal grinding factor ($\mathrm{kg\,h^{-1}\,mm^{-1}\,kW^{-1}}$): 40 for corn and 56 for soybean meal. Both values are adopted from the sectoral tabulation reported in [48] and used in [9]; they do not originate from the 2015 industrial campaign and constitute the external reference basis of the indicator. With $\phi = 3$ mm, the resulting values are $W_{i,\mathrm{ref}} = 8.33$ and 5.95 kWh/t, respectively. The reference grinding power is calculated using Bond's formulation given in Equation (5):

$$P_{\mathrm{grinding}} = \dot{m}\ 0.3162\ W_{i,\mathrm{ref}}\ \frac{1}{\sqrt{D_{pb}}}, \qquad \eta_{\mathrm{proc}} = \frac{P_{\mathrm{grinding}}}{P_{\mathrm{shaft}}}, \tag{5}$$

with $\dot{m}$ expressed in t/h and $D_{pb} = \phi$ in mm. The calculation follows three conventions established by the SFT methodology. First, the reference index is obtained from tabulated values corresponding to the processed material and is not derived from the measured energy consumption. This preserves the normalization of the indicator with respect to a sectoral benchmark while maintaining sensitivity to load effects. Second, the feed particle size term $1/\sqrt{D_{pa}}$ from Bond's equation is omitted according to the SFT convention. This increases the reference energy demand and, consequently, the resulting efficiencies should be interpreted as upper-bound performance indicators. Third, the resulting indicator is defined as a normalized performance ratio, derived from the relationship between the sectoral reference specific energy consumption and the actual shaft specific energy consumption, rather than as an absolute thermodynamic efficiency. Therefore, its numerical value depends on the adopted reference basis, which must be explicitly declared when establishing comparisons. A direct corollary, relevant to the interpretation of Table 4, is that units processing different materials are normalized against different reference bases and are therefore not strictly comparable with one another; the valid comparison is the intra-machine one, between load conditions of the same unit processing the same material. From this definition, the follow-

ing algebraic equivalence can be established: $\eta_{\text{proc}} = 0.3162\, W_{i,\text{ref}}/(\sqrt{D_{pb}}\,\text{SEC}_{\text{shaft}})$, where $\text{SEC}_{\text{shaft}} = P_{\text{shaft}}/\dot{m}$ is the shaft specific energy consumption (kWh/t). Consequently, normalized efficiency and specific energy consumption are not independent evidence sources but rather the same measured quantity expressed on two different scales (Section 3.3).

Table 4. Stage and global efficiencies, current ratios, and power demand of the mechanical SEUs (600 t/day).

Equipment	P_{elect} (kW)	η_{motor}	η_{trans}	η_{proc}	η_{global}	k_I
Hammer Mill IV	98.19	0.92	–	0.286	0.263	0.74
Hammer Mill II	98.19	0.91	–	0.289	0.263	0.74
Hammer Mill III	62.19	0.90	–	0.311	0.279	0.47
Screw conveyor	2.03	0.825	0.85	0.247	0.173 ‡	0.60
Bucket elevator	5.89	0.87	0.832	–	0.724 ‡	0.42

η_{proc} is evaluated at the shaft level; for hammer mills, it is normalized to the SFT reference index and is an upper-bound indicator (Section 2.7.1). Hammer mills use direct drive ($\eta_{\text{trans}} \approx 1$); for the bucket elevator, gravitational lifting constitutes the useful work ($\eta_{\text{proc}} \approx 1$). ‡ Conditional on the adopted nominal throughput (Table 2).

The fixed reference basis also represents a deliberate methodological correction with respect to the calculation procedure used in the 2015 campaign. In that procedure, the grinding factor was derived case by case from the measured shaft power, according to $JKM = \dot{m}/(\phi\, P_{\text{shaft}})$, meaning that the resulting specific energy index became algebraically identical to the measured specific energy consumption, $W_i = P_{\text{shaft}}/\dot{m}$. Substituting this identity into the efficiency definition caused the indicator to collapse into the constant $\eta_{\text{proc}} = 0.3162/\sqrt{\phi}$—approximately 18.3% for $\phi = 3$ mm—a value determined only by the screen size and independent of equipment type, processed material, and throughput. Such a circular indicator cannot capture load effects or discriminate between different units. Therefore, the present study adopts fixed reference values that are material-specific and independent of measured electrical power, thereby eliminating circularity and restoring the diagnostic sensitivity of the indicator. The temperature correction factor (K_t) and hammer-wear correction factor (K_d) from the validated model reported in [9] are included when the measurement campaign provides sufficient characterization data; in the present case study, both factors are assumed to be equal to unity.

2.7.2. Bucket Elevator

The mass per bucket and the transported mass flow rate, according to classical bulk solids-handling models [58,67–69], are determined using Equation (6):

$$M = i\,\rho\,j, \qquad Q = \frac{3.6\,M\,v}{t} \tag{6}$$

where i is the bucket volume (L), ρ is the bulk density (kg/L), j is the filling coefficient (0.6–0.9), v is the belt velocity (m/s), and t is the bucket spacing ($t = 2h$ or $3h$, where h is the bucket height). Using the parameters reported in Table 2 ($M = 6.3 \times 0.82 \times 0.70 = 3.62$ kg; $v = 1.10$ m/s; $t = 0.42$ m $= 2h$), Equation (6) reproduces the nominal throughput of 34 t/h adopted in Table 3. The useful power is defined in a physically unambiguous manner as the gravitational lifting power, according to Equation (7):

$$P_{\text{useful}} = \frac{\dot{m}\,g\,H}{3.6 \times 10^6} \tag{7}$$

where $\dot{m}$ is expressed in kg/h, $g = 9.81$ m/s^2, and H is the lifting height (m). The load-drag resistances—represented in design practice by the equivalent height H_0—together with

belt friction and gearbox losses, are grouped within the transmission stage, as expressed in Equation (8):

$$\eta_{\text{trans}} = \frac{P_{\text{useful}}}{P_{\text{shaft}}} \qquad \eta_{\text{global,elev}} = \eta_{\text{motor}} \cdot \eta_{\text{trans}} \tag{8}$$

where P_{shaft} is obtained from Equation (2). Unlike equipment sizing formulations—which include H_0 and safety margins of 10–20% in the drive power calculation—this definition strictly separates useful work from engineering allowances, preventing design margins from being classified as useful output. It should be noted, however, that η_{trans} is obtained here as a balance-closure term: in addition to H_0 and actual mechanical losses, it incorporates any bias associated with the adopted throughput or the nominal motor efficiency. Therefore, it should be interpreted as the aggregated non-useful fraction of shaft power rather than as a detailed diagnosis of individual transmission components.

2.7.3. Screw Conveyor

The transported throughput and maximum rotational speed, according to the classical mechanics of screw conveying, bulk solids theory, and design standards [70–74], are expressed by Equation (9):

$$Q = 60\,\frac{\pi D^2}{4}\,p\,\psi\,\rho_t\,K\,n, \tag{9}$$

where D is the screw diameter (m), p is the screw pitch (m), ψ is the cross-sectional filling coefficient, ρ_t is the bulk density of the material (t/m^3), K is the inclination coefficient, and n is the rotational speed (rpm), with Q resulting in t/h. Using the parameters reported in Table 2, Equation (9) reproduces the nominal throughput of 45 t/h adopted in Table 3. The theoretical conveying power requirement is given by Equation (10):

$$P_a = \frac{Q\,L}{367}\,(W_0 + \sin\beta), \tag{10}$$

where L is the conveyor length (m), W_0 is the total resistance coefficient—1.6 for low-abrasiveness materials such as cereal grains, consistent with the filling coefficient $\psi = 0.32$ reported in Table 2—and β is the inclination angle. Mechanical power reaches the screw shaft through a gearbox with efficiency η_{trans}. The process efficiency is defined as the ratio between the theoretical conveying power and the actual power delivered to the screw shaft, as expressed in Equation (11):

$$\eta_{\text{proc}} = \frac{P_a}{\eta_{\text{trans}}\,P_{\text{shaft}}}, \qquad \eta_{\text{global,screw}} = \eta_{\text{motor}} \cdot \eta_{\text{trans}} \cdot \eta_{\text{proc}}. \tag{11}$$

The theoretical power requirement P_a incorporates frictional effects through the parameter W_0, which characterizes the dominant mechanism of screw conveying. Unlike the bucket elevator—where useful work is associated with lifting the material against gravity—the screw conveyor inherently dissipates a considerable fraction of the supplied energy through frictional interactions between the material and the casing. For an inclination angle of $\beta = 5°$, the gravitational contribution, expressed as $\sin\beta/(W_0 + \sin\beta)$, represents only 5.2% of the total theoretical demand. This highlights the predominantly dissipative nature of screw conveying and supports the definition of efficiency in Equation (11) as an appropriate performance indicator.

2.8. Stage-Wise Loss Decomposition

Beyond the global efficiency metric, the proposed methodology quantifies losses at each stage of the energy conversion chain. The total dissipated power is calculated as

$L_{\text{tot}} = P_{\text{elect}}(1 - \eta_{\text{global}})$ and distributed among the conversion stages according to the multiplicative structure of the conversion process, as expressed in Equation (12):

$$\begin{aligned} L_{\text{motor}} &= P_{\text{elect}}(1 - \eta_{\text{motor}}), \\ L_{\text{trans}} &= P_{\text{elect}}\,\eta_{\text{motor}}(1 - \eta_{\text{trans}}), \\ L_{\text{proc}} &= P_{\text{elect}}\,\eta_{\text{motor}}\,\eta_{\text{trans}}(1 - \eta_{\text{proc}}), \end{aligned} \tag{12}$$

such that $\sum_i L_i + P_{\text{useful}} = P_{\text{elect}}$. The contribution of each stage to the total losses is defined as $\phi_i = L_i / L_{\text{tot}}$. This formulation enables the identification of the dominant dissipation mechanisms for each equipment category and supports the prioritization of improvement actions, whether operational or technological.

2.9. Equipment-Level Calculation Procedure

The evaluation of each SEU follows a unified calculation sequence, independent of equipment type, ensuring the consistent application of the proposed framework. First, the electrical input power is determined from the operating variables (V_L, I_L, $\cos\varphi$) using Equation (1). The shaft power is then estimated from the rated nameplate efficiency, complemented by the normalized values from the relevant reference standards [56,57], according to Equation (2).

The useful power is subsequently calculated using the physical model corresponding to each equipment category: Bond's comminution theory normalized to the SFT reference for hammer mills (Equations (4) and (5)), the gravitational lifting model for the bucket elevator (Equation (7)), and the theoretical conveying power model for the screw conveyor (Equation (10)). The integration of these elements establishes the complete electrical-to-useful energy conversion chain and enables the estimation of stage-wise efficiencies and global efficiency under actual operating conditions through Equation (3).

Finally, the total dissipated energy is allocated among the conversion stages using Equation (12). Therefore, the procedure provides not only a global efficiency value but also a loss breakdown capable of locating inefficiencies throughout the conversion chain. When data are available for different production levels, the procedure is repeated for each operating condition, allowing load-dependent effects to be distinguished from equipment-inherent limitations. By relying exclusively on field-measurable variables and basic geometric parameters, the methodology can be transferred to other industrial environments with reproducibility and adaptability across different process configurations.

The correspondence between this calculation sequence and the three phases of Figure 1 is direct: the identification of the SEU belongs to Phase 1; Equations (1)–(3) together with the machine-specific useful power model constitute Phase 2; and the stage-wise loss allocation of Equation (12), the uncertainty treatment of Equation (13), and the recoverable-versus-intrinsic classification of the dominant losses complete Phase 3. Figure 1 displays the principal equations within the quantitative blocks, while the present paragraph provides the complete equation-to-phase mapping.

2.10. Uncertainty Analysis and Proposed Inferential Design

The proposed framework is complemented by an uncertainty quantification layer and by the specification of the inferential design required for future statistical validation. The former is directly applied in the present case study (Section 3.5), propagating the combined standard uncertainty of each efficiency metric from the measured quantities through Equation (13). The latter—which requires a multi-load measurement campaign and is not performed in this study—is specified as part of the methodological framework, consistently with the validation strategy adopted for the hammer mill model, which employed ANOVA, ANCOVA, and multiple regression with $R^2 = 0.98$ [9]. The appropriate

experimental design is factorial, crossing equipment type (hammer mill, bucket elevator, screw conveyor), load level λ—with several operating points between no-load and rated operation—and material (corn, soybean meal), with replicated measurements for each experimental cell. After verifying normality (Shapiro–Wilk) and homoscedasticity (Levene's test), a two-way ANOVA and an ANCOVA with load as a covariate would allow the effects of operating regime to be separated from the intrinsic behavior of each equipment category, supported by Tukey post hoc comparisons. The efficiency–load relationship would be modeled through linear and exponential regressions of η_{global} versus λ, reporting R^2, RMSE, and confidence intervals, while the relative influence of operating variables (throughput, particle size distribution, and moisture content) would be quantified using Pearson and Spearman correlation coefficients.

This inferential layer, combined with uncertainty propagation and, when appropriate, Monte Carlo simulation ($N \geq 10^4$) over the distributions of V_L, I_L, $\cos\varphi$, and $\dot{m}$, provides metrological traceability to the diagnostic results. Assuming uncorrelated input variables, the combined standard uncertainty of the efficiency metric is propagated according to Equation (13):

$$\left(\frac{u_\eta}{\eta}\right)^2 = \left(\frac{u_V}{V_L}\right)^2 + \left(\frac{u_I}{I_L}\right)^2 + \left(\frac{u_{\cos\varphi}}{\cos\varphi}\right)^2 + \left(\frac{u_{\dot{m}}}{\dot{m}}\right)^2, \tag{13}$$

and is reported as expanded uncertainty at a 95% confidence level ($k = 2$). Four systematic sources are explicitly identified and addressed through sensitivity analysis or qualitative bounding: the dependence of grinding efficiency on the sectoral reference index (Section 2.7.1), the use of motor nameplate efficiency and rated power factor under partial-load conditions, the adoption of nominal throughputs for bulk solids-handling equipment, and the documentary uncertainty associated with the inherited 5 t/h throughput value (Sections 2.3 and 3.5).

3. Results

3.1. Energy Characterization and Operating Regime

The plant was monitored under three daily production levels. The resulting electrical consumption and energy performance indicators (EnPIs) were 7924.7 kWh at 600 t/day (13.2 kWh/t), 4508.2 kWh at 360 t/day (12.5 kWh/t), and 2157.5 kWh at 100 t/day (21.6 kWh/t). The daily plant records range between 10 and 27 kWh/t, encompassing the sectoral range of 16–22 kWh/t reported for European feed mills with different production capacities [48]. The grinding section accounts for 48% of the total electricity consumption, while pelleting contributes an additional 28%, together representing 76% of the plant demand (Figure 2). The analyzed equipment operates under partial-load conditions, with current ratios k_I of 74% for Hammer Mills II and IV, 47% for Hammer Mill III, 60% for the screw conveyor, and 42% for the bucket elevator. Therefore, the production line operates below the nominal capacity of the installed equipment, and this operating regime plays a significant role in the trends discussed below.

3.2. Equipment Efficiency and Stage-Wise Loss Decomposition

The methodology described in Section 2.9 was applied to the electrical and process measurements reported in Tables 1–3. The stage efficiencies and resulting global performance indicators are summarized in Table 4, which provides the quantitative basis for evaluating the energy conversion behavior of the analyzed equipment.

The results in Table 4 reveal three clearly differentiated performance patterns. The bucket elevator achieves the highest global efficiency ($\eta_{\text{global}} = 72.4\%$), supported by a motor efficiency of 87% and a transmission efficiency of 83.2%. This result is consistent with its operating principle, since the useful output is directly associated with lifting the

material against gravity. It should be noted that this value is conditioned by the assumed nominal throughput (Table 3): if the actual throughput were lower than the design value—a plausible scenario given the current ratio of 0.42—the global efficiency of the elevator would be overestimated in direct proportion, an aspect further addressed in Section 3.5 and the limitations discussion.

Both the bucket elevator and the screw conveyor efficiencies reported in Table 4 are conditional on the adopted nominal throughput, since no in-line gravimetric measurement was available for either unit (Section 2.3); they are therefore not directly comparable, in metrological status, with the hammer mill values, which are based on throughputs traceable to plant production records. The plausible range of the bucket elevator efficiency under the two coupled systematic biases is quantified in Section 3.5 and spans 43–89%, so that the 72.4% point estimate should not be adopted as a fixed reference for this equipment class.

The screw conveyor exhibits a different behavior: its global efficiency is considerably lower ($\eta_{\text{global}} = 17.3\%$), with a process performance ratio of 24.7% considering a motor efficiency of 82.5% and gearbox efficiency of 85%. This level is explained by the dissipative nature of screw conveying, where internal friction and interactions between the transported material and the equipment consume a substantial fraction of the supplied energy.

Although the hammer mills are equipped with high-efficiency motors (90–92%), their global efficiencies range between 26.3 and 27.9%. At the process stage, efficiencies vary from 28.6 to 31.1% at the shaft level normalized to the SFT reference, and therefore should be interpreted as conservative upper bounds. These values are consistent with the inherently low efficiency of size-reduction processes, in which only a small fraction of the supplied energy contributes directly to particle breakage even under appropriate operating conditions [62,66]. It must be noted that Hammer Mill III processes soybean meal and is therefore normalized against a different reference index ($W_{i,\text{ref}} = 5.95$ kWh/t) than Mills II and IV, which process corn ($W_{i,\text{ref}} = 8.33$ kWh/t). The three process efficiencies are consequently not strictly comparable with one another (Section 2.7.1); the load-dependent comparison reported in Section 3.3 is intra-machine and does not suffer from this restriction.

Overall, the results indicate that motor efficiency is not the main limitation of the analyzed equipment: the dominant losses occur in the downstream conversion stages associated with the physical transformation of the material.

3.3. Evaluation Under Different Load Levels

Because grinding efficiency depends on throughput, the methodology was applied at three production levels, explicitly distinguishing between plant load (daily production) and machine load (instantaneous equipment throughput), which do not necessarily coincide: at 100 t/day, the mills operated fewer hours but at full instantaneous load (16–17 t/h), whereas at 360 t/day, Hammer Mill III operated underfed at 5 t/h during the soybean processing campaign.

Before presenting the results, the metrological status of the 5 t/h operating point must be clarified. This throughput value originates from inherited records of the 2015 campaign, whose documentation for the 360 t/day scenario presents internal inconsistencies between daily production, operating hours, and instantaneous throughput (Section 2.3); therefore, it is treated as inherited data with documentary uncertainty. For the electrical demand of Hammer Mill III under this condition, the measured current value of 95 A is adopted ($P_{\text{elect}} = 62.19$ kW; $P_{\text{shaft}} = 55.97$ kW with $\eta_{\text{motor}} = 0.90$), as this is the only electrical measurement available for this unit. This assumption bounds the result in a defined direction: if the actual current under partial-load operation were lower than the recorded value, the specific energy consumption would be lower and the efficiency higher than the reported value; consequently, the 9.7% value represents a lower bound of efficiency under

the underfed condition. The existence and direction of the efficiency deterioration with reduced loading are therefore supported; its exact magnitude remains conditioned by the traceability of the inherited throughput, a limitation further discussed in Section 4.

Figure 3 summarizes both effects on a common basis: panel (a) presents the plant EnPI for the three monitored production levels, while panel (b) shows the process efficiency of Hammer Mill III and its shaft specific energy consumption as a function of machine throughput.

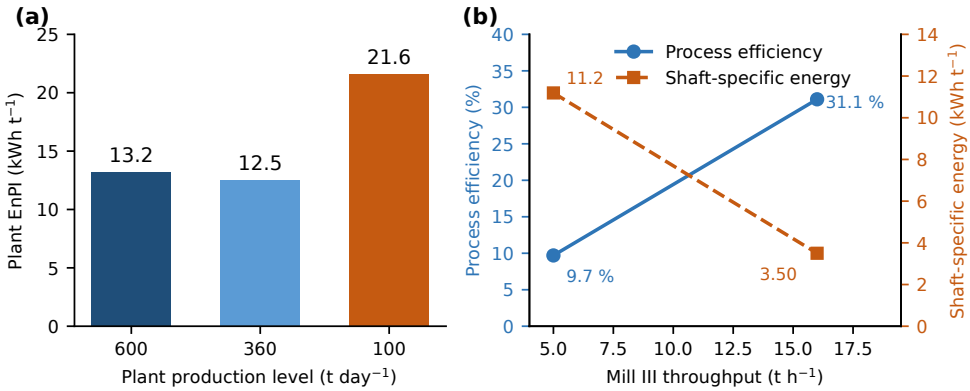

Figure 3. Effect of operating load on energy performance. (**a**) Plant EnPI for the three monitored production levels. (**b**) Process efficiency and shaft specific energy consumption of Hammer Mill III versus throughput.

The combined analysis of both panels highlights two relevant findings. First (panel b), grinding efficiency exhibits a clear dependence on operating load: Hammer Mill III, processing soybean meal, reaches a process efficiency of 31.1% at 16 t/h, which decreases to 9.7% when throughput is reduced to 5 t/h. This variation is associated with the change in operating condition, since motor characteristics and processed material remain constant. The measured shaft specific energy consumption increases from 3.50 to 11.2 kWh/t as throughput decreases (ratio 3.20). It is important to clarify the status of both quantities: according to the algebraic equivalence established in Section 2.7.1, normalized efficiency is the scaled reciprocal of shaft specific energy consumption. Therefore, the decrease from 31.1→9.7% and the 3.20 increase in specific energy consumption do not constitute independent evidence, but rather represent the same measurement expressed on two different scales. The primary magnitude is the specific energy consumption; the normalized efficiency adds comparability against the sectoral reference and enables integration within the conversion chain described by Equation (3).

Second (comparison between panels), the plant EnPI exhibits the opposite trend to equipment-level efficiency: it deteriorates at 100 t/day (21.6 kWh/t, with fixed auxiliary loads distributed over fewer tonnes) despite the mills operating at full instantaneous load, and improves at 360 t/day (12.5 kWh/t) despite the underfed operation of Hammer Mill III. Therefore, plant underloading and machine underloading are distinct phenomena with opposite energy signatures, and only stage-wise decomposition at the equipment level allows them to be separated: an aggregated indicator systematically masks this difference.

An additional clarification applies to the 100 t/day scenario: in the inherited records, equipment power values correspond to punctual operating measurements, whereas daily energy values originate from averaging periods that do not exactly coincide with nominal operating hours. Therefore, instantaneous power, daily energy, and nominal operating time should not be combined as if they described a single stationary condition. In this study, the 100 t/day scenario is used exclusively for the plant EnPI evaluation shown in panel (a), and is not employed for equipment-level efficiency calculations.

3.4. Localization of Losses Along the Energy Conversion Chain

The allocation of dissipated power among the successive conversion stages using Equation (12) produces the results summarized in Table 5. These results represent the central conceptual outcome of the demonstration: the transition from a scalar efficiency indicator to a localized loss profile along the complete energy conversion chain.

Table 5. Stage-wise loss decomposition under operating conditions: losses by conversion stage (kW) and useful power output. Hammer mills are direct-drive systems ($\eta_{\text{trans}} \approx 1$).

Equipment	L_{motor}	L_{trans}	L_{proc}	P_{util}	η_{global}
Hammer Mill IV	7.86	0.00	64.47	25.86	0.263
Hammer Mill II	8.84	0.00	63.50	25.86	0.263
Hammer Mill III	6.22	0.00	38.59	17.38	0.279
Screw conveyor	0.36	0.25	1.07	0.35	0.173
Bucket elevator	0.77	0.86	–	4.27	0.724

The results in Table 5 illustrate how energy losses are distributed among the conversion stages of each equipment category. In hammer mills, the process stage concentrates the largest fraction of the dissipated power: Hammer Mill IV presents total losses of 72.3 kW, of which 64.5 kW correspond to the process stage (approximately 89%), whereas motor losses remain comparatively low (7.9 kW). The screw conveyor exhibits a similar pattern, with 1.07 kW of its 1.68 kW total losses attributed to the process stage. The bucket elevator, in contrast, shows a lower overall dissipation level, with losses more evenly distributed; under the adopted framework, these losses are assigned by definition to the motor and to the aggregated transmission term, which incorporates the equivalent loading height and mechanical resistances (Section 2.7).

The stage-wise loss analysis demonstrates that equipment efficiency cannot be reliably assessed from motor performance alone. Even when motors operate within a high-efficiency range (90–92%), global efficiency decreases substantially when most of the supplied energy is dissipated downstream of the motor, during the conversion of shaft power into useful process output. This level of detail cannot be obtained from aggregated plant indicators or from analyses limited exclusively to the electrical drive system. By explicitly assigning losses among the successive conversion stages, the proposed methodology enables a more comprehensive evaluation of energy performance and supports the identification of the most effective improvement actions. For hammer mills, this interpretation is further supported by the load-dependent analysis presented in Section 3.3, which allows operational effects to be distinguished from losses inherent to the comminution process.

3.5. Uncertainty and Sensitivity Analysis

The reported efficiencies are expressed as point estimates, and their uncertainty is evaluated by propagating the measurement uncertainties according to Equation (13). Since no specific calibration information was available for the instruments used during the measurement campaign (Section 2.3), representative field measurement uncertainties were assumed: $u_V/V_L = 1.5\%$ and $u_I/I_L = 1.5\%$ for the clamp meter/power analyzer, $u_{\cos\varphi} = 0.02$ over $\cos\varphi = 0.86$ (2.3%), and $u_{\dot{m}}/\dot{m} = 5\%$ for the material flow-rate estimation. Under these assumptions, the combined relative uncertainty of the efficiency calculation is 5.9%, with the dominant contribution arising from the estimation of the material flow rate. The expanded uncertainty at a 95% confidence level ($k = 2$) is therefore 11.8%. This value quantifies the random measurement component under the stated assumptions; systematic sources—including the sectoral reference index, nominal motor parameters under partial-load conditions, nominal flow rates for bulk material-handling equipment,

and the documentary uncertainty associated with the inherited flow-rate value—are not covered by this uncertainty and are addressed separately through the sensitivity analysis presented at the end of this section.

Table 6 presents the uncertainty propagation results for each equipment item, expressed as expanded uncertainty in percentage points of efficiency.

Table 6. Global efficiency with expanded uncertainty at a 95% confidence level ($k = 2$), obtained from Equation (13).

Equipment	η_{global} (%)	U ($k = 2$, p.p.)	$\eta_{\text{global}} \pm U$ (%)
Hammer Mill IV	26.3	3.1	26.3 ± 3.1
Hammer Mill II	26.3	3.1	26.3 ± 3.1
Hammer Mill III	27.9	3.3	27.9 ± 3.3
Screw conveyor	17.3 ‡	2.0	17.3 ± 2.0
Bucket elevator	72.4 ‡	8.6	72.4 ± 8.6

‡ Additionally conditional on the adopted nominal throughput; the systematic component is bounded in Table 7.

The uncertainty ranges reported in Table 6 do not alter the identified performance trends: the hammer mills (26.3–27.9%) and the screw conveyor (17.3%) remain clearly differentiated from the bucket elevator (72.4%), preserving the relative ranking among the analyzed systems. The overlap among the three hammer mills is consistent with their similar operating conditions at 600 t/day and indicates that their performance differences cannot be statistically distinguished within the estimated uncertainty range. Figure 4 illustrates the uncertainty intervals (panel a) and the contribution of each measured variable to the combined uncertainty (panel b).

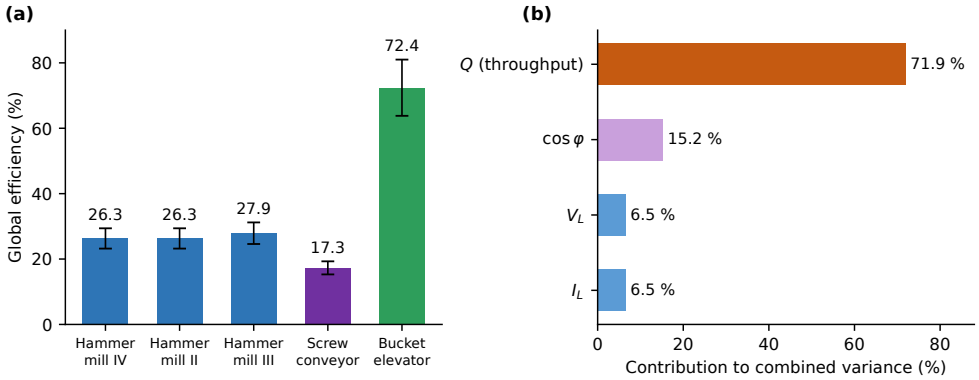

Figure 4. Uncertainty analysis. (**a**) Global efficiency with expanded uncertainty at a 95% confidence level ($k = 2$). (**b**) Contribution of each variable to the combined variance. Values for the screw conveyor and the bucket elevator are conditional on the adopted nominal throughput.

The uncertainty budget shown in panel (b) of Figure 4 indicates that the dominant contribution to the combined variance originates from the estimation of the material flow rate Q, accounting for 71.9% of the total variance. The power factor contributes 15.2%, while voltage and current measurements contribute smaller and equivalent shares of 6.5% each. The metrological implication is direct and is reinforced by the fact that, for the screw conveyor and bucket elevator, the adopted flow rates are nominal values rather than direct measurements (Section 2.3). Therefore, the most effective strategy for reducing diagnostic uncertainty is not improving electrical instrumentation—which is already adequate—but incorporating continuous gravimetric measurement of the processed mass flow.

To verify that the analytical propagation of Equation (13) is not dependent on linearity assumptions, a Monte Carlo simulation was performed according to the framework specified in Section 2.10. A total of $N = 10{,}000$ samples of V_L, I_L, $\cos\varphi$, and $\dot{m}$ were

generated from normal distributions centered on the measured values of Hammer Mill IV. Each realization was propagated through the efficiency model, which—because it is normalized against a tabulated reference index—retains sensitivity to all measured variables ($\eta \propto \dot{m}/(V_L\, I_L\, \cos\varphi)$). The resulting distribution is presented in Figure 5.

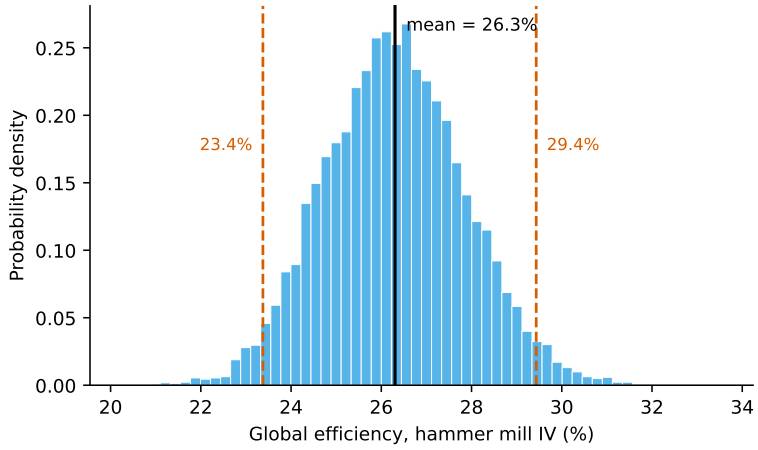

Figure 5. Global efficiency of Hammer Mill IV obtained by Monte Carlo simulation ($N = 10{,}000$). Solid line: mean; dashed lines: 95% confidence interval.

The distribution shown in Figure 5 is approximately symmetrical and centered at 26.3%. The 95% confidence interval ranges from 23.4 to 29.4%, with a relative standard deviation of 5.9%. The agreement with the analytical propagation confirms that, for the assumed measurement precision, the first-order approximation is reliable and that the expanded uncertainty estimate can be considered robust.

A sensitivity analysis was additionally conducted on the declared systematic sources. The first source is the SFT reference index: a variation of $\pm 10\%$ in $W_{i,\mathrm{ref}}$ produces a proportional change in the estimated grinding efficiencies (approximately ± 2.6 to 3.1 percentage points), without modifying the relative ranking of the equipment or the load-dependent trends, which are governed by the measured specific energy consumption. The second source is the assumed power factor: under partial-load operation, the actual $\cos\varphi$ may deviate from its nameplate value. For the bucket elevator ($k_I = 0.42$), assuming an effective $\cos\varphi$ of 0.70 reduces the estimated electrical power to approximately 4.8 kW and increases the global efficiency to nearly 89%; the hammer mills, operating at $k_I = 0.74$, exhibit limited sensitivity to this parameter. The third source is the nominal flow rate adopted for bulk material-handling equipment: unlike the previous factor, this bias acts in the opposite direction for the elevator—a real flow rate lower than the nominal value would proportionally reduce its estimated efficiency. The fourth source is the inherited 5 t/h flow rate of Hammer Mill III, whose uncertainty is documentary and cannot be propagated statistically; its treatment as a bounded estimate is established in Section 3.3.

The second and third systematic sources were analyzed independently in the original formulation, whereas under underfed operation both coexist and act in opposite directions. Table 7 therefore reports the bucket elevator efficiency over the crossed combination of both biases. The reduced-throughput scenario was set at 20 t/h (59% of the nominal value) as a reasonable lower bound; the product $k_I\, Q_{\mathrm{nom}} = 14.3$ t/h was not adopted because, as established in Section 2.4, k_I does not constitute a mechanical load factor and overstates the reduction in useful power demand.

Table 7. Bucket elevator global efficiency under the crossed combination of the two systematic biases of opposite sign.

Assumed $\cos\varphi$	$Q = 34$ t/h (Nominal)	$Q = 20$ t/h (Underfed)
0.86 (nameplate)	72.4%	42.6%
0.70 (partial load)	89.1%	52.4%

$P_{\text{useful}} = 4.27$ kW at 34 t/h and 2.51 kW at 20 t/h (Equation (7)); $P_{\text{elect}} = 5.89$ kW at $\cos\varphi = 0.86$ and 4.80 kW at $\cos\varphi = 0.70$ (Equation (1)), $I_L = 9.0$ A).

Taken jointly, the two systematic biases bound the bucket elevator efficiency within the interval 43–89%. This interval is wide, and the 72.4% point estimate should therefore not be used as a fixed reference for this equipment class without direct gravimetric and power measurement. What the interval does preserve is the ordinal diagnosis: even at its lower bound (42.6%), the bucket elevator remains well above the hammer mills (26.3–27.9%) and the screw conveyor (17.3%). The equipment ranking—which is the output on which the decision structure of Figure 1 operates—is therefore robust to both systematic sources, whereas the cardinal value is not. This conditionality is furthermore confined to the bulk solids-handling equipment: the hammer mill diagnosis rests on throughputs traceable to plant production records (Section 2.3, level (i)) and is unaffected. None of these scenarios modifies the ranking among equipment items or the diagnosis of the dominant losses in the hammer mills.

It should be emphasized that the Monte Carlo simulation is used exclusively to evaluate the propagation of measurement uncertainty and does not replace inferential statistical analysis. The methods outlined in Section 2.10—ANOVA, ANCOVA, and efficiency–load regression—require a broader experimental dataset covering a wider range of operating conditions. Expanding this dataset is therefore identified as a priority for future research.

4. Discussion

The main outcome of this study is the explicit differentiation between motor efficiency and overall equipment efficiency. This finding challenges the common assumption that poor energy performance originates primarily in the electrical drive system: traditional efficiency strategies tend to focus on motor replacement or variable-speed drive installation, whereas the stage-resolved analysis indicates that the hammer mills—the largest electricity-consuming units in the plant—are already equipped with motors operating at 90–92% efficiency. Most of the losses occur downstream of the motor, during the conversion of shaft power into the mechanical work required for particle size reduction. The main limitation therefore lies in the process stage rather than in the drive system, a distinction that cannot be established through aggregated energy indicators or analyses restricted to motor performance alone.

Evaluating electrical-to-useful efficiency throughout the sequence of energy conversion stages provides a more comprehensive understanding of equipment performance. Beyond quantifying total losses, the proposed framework identifies where these losses occur, enabling the selection of improvement measures aligned with their origin: operational, technological, or intrinsic to the process. The analysis also reveals an aspect that conventional indicators fail to capture: the distinction between plant underloading and equipment underloading, which exhibit opposite energy-performance behaviors (Section 3.3); when this distinction is neglected, aggregated metrics may lead to misleading interpretations of performance. The following discussion contextualizes these findings within the existing literature, examines the three efficiency regimes identified, and defines the scope of this single-case study.

4.1. Positioning with Respect to the State of the Art

Table 8 positions this work relative to previous research lines. The closest contributions are energy analyses conducted in feed mills. Crespo Sánchez et al. [3] determined, in a feed production plant, the motor efficiencies of conveyors, elevators, and screw feeders under their actual load factors and implemented ISO 50001 indicators (energy intensity of 10 kWh/t, with reported savings of 15%); however, their analysis is restricted to motor efficiency and does not decompose the subsequent conversion stages. Sakthivel et al. [75] compared specific energy consumption against benchmark values in three commercial plants, but only at feed-type level rather than at equipment level. More recent manufacturing-level studies report persistent energy-performance improvements under ISO 50001-based systems and examine the relationship between energy-information systems and ISO 50001 energy-management architectures [43,44]. These contributions strengthen the contemporary energy-management context, but remain at the organizational or management-system level rather than decomposing electrical-to-useful efficiency by equipment stage.

In parallel, classical comminution theory [62–64] and grinding studies [19,76,77] model the energy demand of the particle size reduction process, whereas screw conveyor literature [70,72,74,78], including recent reviews of DEM-based analysis [33], provides design power requirements and volumetric efficiencies for bulk material transport, without integrating these elements into a unified electrical-to-useful efficiency framework. The advanced hammer mill model reported by Castillo Alvarez et al. [9] provides a field-validated formulation, but it is restricted to a single equipment type.

Table 8. Comparison with representative studies on energy analysis and modeling in feed mills, bulk solids handling, and comminution equipment. HM: hammer mill; BE: bucket elevator; SC: screw conveyor; SEC: specific energy consumption; PSD: particle size distribution; EnPI: energy performance indicator. Last column: Y = yes (all four attributes); P = partial; N = no.

Study	Equipment	Approach	Main Result/Focus	Unified, Stage-Based, Field Applicable
Energy analysis in feed mills				
[3]	Feed mill	Motor efficiency + EnPI (ISO 50001)	Conveyors, bucket elevators, screw conveyors; EnPI of 10 kWh/t, 15% energy savings	P (motor only, no stage-wise decomposition)
[75]	Feed mills (×3)	Energy benchmarking	SEC by feed type in three commercial plants	N
[43,44]	Manufacturing/EnMS	ISO 50001 and energy-information systems	Persistent energy-performance improvement and management-system architecture	N (plant/management-system level)
[48]	Feed mill	SFT methodology	Grinding factors and reference energy consumption by grain/screen size	P (sectoral benchmark, no conversion chain)
Grinding: theory, energy, and size reduction				
[62–64]	Hammer mill	Comminution theory	Energy–size reduction laws	N
[10,11]	Hammer mill	Experimental	SEC as a function of rotor speed and screen size	N
[12,13]	Hammer mill	Experimental	Energy demand versus material properties and moisture content	N
[19]	Hammer mill	Comparative study	Specific energy by mill type	N
[25,76,77,79]	Hammer mill	Modeling/experimental	PSD, work index, screen size, and moisture effects	N
[29]	Hammer mill	CFD–DEM + experiment	Effects of speed, hammer–screen gap, and screen aperture on grinding performance	N
[26,27]	Pellet mill	Conditioning	Energy demand and pellet quality	N
bulk solids-handling systems				
[70]	Screw conveyor	Theory/performance	Vortex flow and volumetric efficiency	N
[71,72,74]	Screw conveyor	DEM/standards	Capacity, power demand, dissipation, and design power	N
[33,38,78]	Screw conveyor	Theoretical/experimental/DEM review	Optimum conveying capacity and power demand; consolidated effect of speed, inclination, and fill level	N
[58,67]	Bucket elevator	Manuals/standards	Lifting power and design rules	N
Validated models and authors' contributions				
[9]	Hammer mill	Validated model (K_t, K_d)	Hammer mill model: $R^2 = 98\%$, 18% reduction in energy consumption	P (hammer mill only)
[47]	Bioenergy systems	Diagnosis/simulation	Agro-industrial energy systems	P
This work	HM/BE/SC	Stage-based, field-measurable methodology	Hammer mills 26–28%, bucket elevator 72%, screw conveyor 17%; load-induced collapse from 31→10%	Y

No previous study simultaneously combines the attributes identified in the final row of Table 8: coverage of heterogeneous high-consumption equipment, stage-wise efficiency de-

composition, a unified field-measurable procedure, and application using real operational data. This constitutes the methodological gap addressed by the proposed framework.

The comparison in Table 8 shows that the three main research domains—plant energy management, comminution theory, and bulk solids handling—have largely evolved independently. Each examines a specific segment of the energy conversion chain in depth, yet none follows the complete pathway from electrical input to useful process output. This observation explains the final row of the table: rather than replacing existing methodologies, the proposed framework integrates them under a common electrical-to-useful efficiency metric decomposed into successive conversion stages.

4.2. Equipment-Level Interpretation

The equipment-level analysis reveals three distinct performance regimes that are not apparent from aggregated energy indicators. The bucket elevator achieves the highest global efficiency (72.4%) when useful work is defined strictly as gravitational lifting. This value is conditional: under the crossed systematic-bias scenarios of Table 7 it ranges between 43 and 89%, and it is the ordinal position of the elevator—not its cardinal value—that supports the management conclusion drawn below. The result is consistent with the operating principle of bucket elevators, in which most of the supplied energy is converted directly into vertical material transport while frictional losses remain comparatively limited [58]. Under these conditions, the potential for additional energy savings is therefore relatively small.

The screw conveyor exhibits a markedly different behavior. Although both the motor and the transmission operate with relatively high efficiencies, the process efficiency remains low (24.7%), reflecting the intrinsic characteristics of screw conveying. Friction against the casing, internal recirculation, and the complex flow behavior of bulk solids dissipate a substantial fraction of the supplied mechanical energy [70,72]. These losses should therefore be interpreted as inherent to the conveying mechanism rather than as evidence of poor operation. At an inclination angle of 5°, only 5.2% of the theoretical power demand is associated with gravitational transport, implying that substantial efficiency improvements would require changes in conveyor design or configuration rather than modifications to the drive system.

The hammer mills display a third performance regime. Despite motor efficiencies of 90–92%, most of the energy losses are concentrated in the process stage, whose performance is strongly dependent on operating load. This dependence becomes evident when the operating conditions change: the process efficiency of Hammer Mill III decreases from 31.1% at 16 t/h to 9.7% at 5 t/h, while the shaft-specific energy consumption increases from 3.50 to 11.2 kWh/t. Given the observed current ratios (0.47–0.74), part of this deterioration is attributable to operation below the design capacity and could potentially be mitigated through improved feed control and load management. The remaining losses, however, are intrinsic to the comminution process itself.

4.3. Implications for Energy Management

From an energy management perspective, the stage-wise decomposition of energy losses provides a structured basis for prioritizing improvement actions in accordance with the principles of ISO 50001 [49,50,52]. For the hammer mills, which account for the largest share of electricity consumption, motor replacement is unlikely to yield significant benefits because the installed motors already operate at high efficiencies. Greater improvements are expected from maintaining operation close to the nominal throughput and avoiding underfed conditions such as the 5 t/h operating point observed for Hammer Mill III. This

objective may be achieved through improved feed control strategies, including the use of variable-frequency drives in dosing systems [40].

For the screw conveyor, the analysis indicates that substantial efficiency gains would require redesign or replacement of the conveying system rather than operational adjustments. In contrast, the bucket elevator does not appear to require major intervention. Establishing this hierarchy of actions—what should be improved, where intervention is required, and whether the solution is operational or technological—is not possible using aggregated plant-level energy indicators alone [3]. This capability therefore represents one of the principal strengths of the proposed framework as an equipment-level energy management tool.

The stage-wise decomposition also supports the conventional intervention hierarchy, which proceeds from the end-use side towards the supply side in increasing order of capital intensity. In the present case the diagnosis places the highest-value action at the lowest-cost end of that hierarchy: throughput stabilization of the hammer mills is an operational measure requiring feed-control adjustment rather than capital replacement, whereas the drive-side measures conventionally prioritized—motor replacement or variable-speed drives on the mill drives—address a stage that accounts for only about 11% of the losses of the dominant SEU. It is precisely this reordering of priorities, and not the absolute efficiency values, that constitutes the practical output of the framework.

4.4. Extension of the Framework to the Pelleting Stage

Pelleting represents 28% of the plant electricity demand (Figure 2) and was excluded from the present analysis for instrumentation reasons, not structural ones. Extending the framework to this stage requires no change in its architecture—the cascade of Equation (3) remains valid—but it does require a redefinition of P_{useful}, because conditioning introduces a thermal energy input that the electrical chain does not capture. Three additions are necessary.

(i) Thermal boundary: steam mass flow rate and specific enthalpy at the conditioner inlet, together with the inlet and outlet temperature and moisture content of the mash, so that the thermal input can be quantified independently of the electrical input and both carriers reported as separate specific energy consumptions ($\text{kWh}_\text{e}/\text{t}$ and $\text{kWh}_\text{th}/\text{t}$). (ii) Mechanical boundary: absorbed power of the main pellet-mill motor under load and at no load, roller–die gap, and die compression ratio (L/D), which govern the extrusion work per unit mass. (iii) Useful-output definition: the useful work of pelleting is the compaction work required to reach the target durability, so that P_{useful} must be referenced to a product-quality benchmark—pellet durability index (PDI) and fines fraction—rather than to a purely geometric criterion. Under this definition, η_{proc} for the pellet mill becomes a quality-normalized performance ratio, structurally analogous to the SFT-normalized ratio adopted here for hammer mills (Section 2.7.1).

It should be noted that ambient climatic normalizers such as heating or cooling degree-days, appropriate for space-conditioning loads, are not suitable drivers for this stage: the dominant relevant variables are the steam mass flow rate and enthalpy, the formulation, and the inlet moisture content, while ambient temperature intervenes only marginally through the initial temperature of the material. Adopting a degree-day normalizer here would introduce a non-causal variable into the energy baseline in the sense of ISO 50006 [51]. The instrumentation required for the extension—steam flow meter, in-line moisture probe, and a three-phase power logger on the main drive—was not available during the 2015 campaign, which is the reason for the exclusion.

4.5. Limitations

Several limitations should be acknowledged. The demonstration is based on a single feed mill and three operating conditions rather than on a controlled load sweep. Consequently, the efficiency–load relationship is characterized only at discrete operating points—including only two conditions for Hammer Mill III—and is not modeled over its full operating range. For this reason, the multi-condition experimental campaign and statistical analysis described in Section 2.10 remain necessary for comprehensive validation.

The underlying data originate from an industrial measurement campaign conducted in 2015, whose original documentation does not report the instrument models, measurement accuracies, calibration status, or sampling frequency. The representative instrumental uncertainties assumed in Section 3.5 only partially compensate for this limitation. The nameplate-based determination of P_{elect} is, in fact, the principal metrological weakness of this demonstration. It is inherited from the legacy campaign and is not a feature of the proposed framework, which specifies integrated power logging as the required measurement level (Section 2.3). In particular, the archived records for the 360 t/day operating condition contain internal inconsistencies between daily production, operating hours, and instantaneous throughput. The 5 t/h throughput reported for Hammer Mill III is therefore treated as a historical value with documentary uncertainty. Although the existence and direction of the efficiency deterioration under partial loading are supported by the measured specific energy consumption, the exact magnitude of the observed efficiency collapse remains contingent on recovering the original measurement records.

The grinding efficiency is defined as a performance ratio normalized to the SFT reference work index. Its absolute value therefore depends on the adopted benchmark, although the relative ranking of the equipment and the observed load effects remain robust to this choice, as demonstrated by the sensitivity analysis. Moreover, omission of the Bond feed-size term makes the reported efficiencies conservative upper bounds. By construction, the normalized grinding efficiency and the shaft-specific energy consumption are algebraically equivalent expressions of the same measurement and should not be interpreted as independent lines of evidence. In addition, units processing different materials are normalized against different reference indices and are therefore not strictly comparable with one another.

The conveying rates adopted for both the screw conveyor and the bucket elevator correspond to nominal operating values rather than gravimetric measurements. Consequently, the estimated efficiency of the bucket elevator—which depends directly on the assumed conveying rate—should be regarded as conditional until confirmed through direct flow measurements, with a plausible range of 43–89% under the coupled systematic-bias scenarios of Table 7. Likewise, the current ratio k_I, used as an indicator of operating regime, is not equivalent to the mechanical load factor and tends to overestimate the fraction of useful power delivered under low-load conditions. The use of nominal motor efficiency and power factor values during partial-load operation introduces an additional conservative bias, quantified for the bucket elevator in the sensitivity analysis.

Finally, the results for the screw conveyor and bucket elevator are based on a single representative unit of each equipment type. Their extrapolation to the entire plant, as well as any broader transferability to other industrial facilities, requires additional datasets and field measurements. Likewise, the absence of an established methodology for evaluating the operational efficiency of bulk solids-handling systems in feed mills should ideally be confirmed through a systematic literature review before being stated categorically. The mechanical models adopted here are established formulations, not new contributions; their role is to close the electrical-to-useful chain for each equipment class. Any claim about feed mills as a population—rather than about this facility—would require the multi-plant

campaign specified in Section 2.10 and is explicitly not made in this work. These limitations affect the numerical scope of the case study but do not alter the methodological structure of the proposed framework, which constitutes the primary contribution of this work.

5. Conclusions

A common, field-measurable methodological framework was formalized that repositions energy-efficiency assessment in the feed industry from determining how much energy each unit consumes to identifying where losses occur along the electrical-to-useful energy conversion chain. The framework integrates three sequential phases: (i) characterization and selection of Significant Energy Uses (SEUs) in accordance with ISO 50001; (ii) a unified procedure that decomposes the electrical-to-useful efficiency of each unit into its successive stages—motor, transmission, and process—by coupling the electrical conversion chain with the equipment-specific useful power model; and (iii) application under real operating conditions, including stage-by-stage loss allocation and uncertainty analysis. The framework additionally declares the measurement and verification basis required for its compliant application, in accordance with ISO 50015 (Section 2.3). Its conceptual contribution lies in treating physically heterogeneous equipment—hammer mills, bucket elevators, and screw conveyors—within a common, comparable, and auditable assessment framework, while providing a sector-normalized definition of milling efficiency that, unlike the circular calculation adopted during the original 2015 measurement campaign, preserves sensitivity to operating load.

Application of the framework to the Piensos Cienfuegos feed mill revealed a systematic distinction between motor efficiency and overall equipment efficiency. Although the installed motors operate with high efficiencies (90–92%), the hammer mills achieved global efficiencies of only 26–28% because nearly 90% of the total losses occur in the process stage rather than in the electrical drive. The bucket elevator exhibited the highest overall performance (72.4%; conditional, with a plausible range of 43–89% under coupled systematic-bias scenarios) when useful work was defined exclusively as gravitational lifting, whereas the screw conveyor showed the lowest performance (17.3% global efficiency and a process performance ratio of 24.7%), with only 5.2% of its transport power demand associated with the gravitational component. Milling performance proved to be strongly dependent on operating load: the process efficiency of Hammer Mill III decreased from 31.1% at 16 t/h to 9.7% at 5 t/h—a value representing a lower bound under the stated electrical assumption—corresponding to the normalized expression of the increase in shaft-specific energy consumption from 3.50 to 11.2 kWh/t (ratio 3.20). The multi-load analysis further demonstrated that plant underloading and machine underloading are distinct operating conditions with opposite energy-performance implications, which can only be distinguished through equipment-level stage decomposition. Consequently, the primary improvement opportunity for the hammer mills is not motor replacement—since the motors already operate efficiently—but maintaining material throughput close to the design operating range.

Two boundaries of these findings must be stated unambiguously. First, the efficiency–load relationship reported here rests on two discrete operating points for a single unit (16 and 5 t/h for Hammer Mill III) and does not constitute a characterized efficiency–throughput curve. The direction of the effect is supported by the measured shaft-specific energy consumption; its functional form and its magnitude are not. The inferential design specified in Section 2.10—factorial ANOVA/ANCOVA over a systematic load sweep with replicated measurements—remains a prerequisite for any statistical claim and is not performed in this work. Second, the improvement opportunities identified above—load stabilization for the hammer mills, redesign for the screw conveyor, no intervention

for the bucket elevator—are prioritized outputs of a diagnosis, not verified savings. No retrofit or operational intervention was implemented at the plant, and their quantification would require a measurement and verification exercise in accordance with ISO 50015 over a defined reporting period after implementation.

The principal contribution of this work is therefore not the numerical values obtained for the case study but the methodological framework itself. By linking field electrical measurements with equipment-specific useful power models, the framework enables stage-based efficiency assessment of heterogeneous equipment through a consistent, reproducible, and auditable procedure suitable for industrial energy management applications. Future work should include, as the first priority, systematic load-sweep experiments to fully characterize the efficiency–throughput relationship and support the proposed inferential statistical analysis, followed by direct measurement of motor power factor and efficiency under partial-load operation, implementation of continuous gravimetric throughput measurement—the dominant source of diagnostic uncertainty—integrated power logging on the bulk solids-handling equipment across peak, low-load, and idle regimes, recovery of the original records from the 2015 measurement campaign to strengthen the traceability of the intermediate-load scenario, propagation of the complete uncertainty associated with all underlying indicators, including the sector reference index, extension of the framework to the pelleting stage under the protocol specified in Section 4.4, and application of the methodology to an independent industrial facility in order to strengthen external validation and assess its generalizability.

Author Contributions: Conceptualization, Y.C.A. and R.J.B.; methodology, Y.C.A., R.J.B., J.P.M.Y. and L.A.I.C.; validation, Y.C.A., R.J.B., J.P.M.Y., P.Y.S.-C. and J.R.-R.; formal analysis, Y.C.A., R.J.B., J.P.M.Y., L.A.I.C. and J.R.-R.; investigation, Y.C.A., P.Y.S.-C. and J.B.R.-O.; resources, Y.C.A., J.B.R.-O. and L.A.I.C.; data curation, Y.C.A., R.J.B. and P.Y.S.-C.; writing—original draft preparation, Y.C.A.; writing—review and editing, R.J.B., J.P.M.Y., P.Y.S.-C., J.B.R.-O., L.A.I.C. and J.R.-R.; visualization, Y.C.A. and J.B.R.-O.; supervision, Y.C.A., R.J.B., J.P.M.Y. and J.R.-R.; project administration, Y.C.A. All authors have read and agreed to the published version of the manuscript.

Funding: This research received no external funding.

Institutional Review Board Statement: Not applicable.

Informed Consent Statement: Not applicable.

Data Availability Statement: The data supporting this study originate from an industrial measurement campaign conducted in 2015 at the "Piensos Cienfuegos" feed mill (Cuba) and documented in an undergraduate thesis at the University of Cienfuegos, complemented by the methodological reformulation and calculations developed in the present work. The datasets are available from the corresponding author upon reasonable request.

Conflicts of Interest: The authors declare no conflict of interest.

Abbreviations

The following abbreviations are used in this manuscript:

SEC	Specific energy consumption
PSD	Particle size distribution
EnPI	Energy performance indicator
ISO	International Organization for Standardization
JKM	Milling factor (SFT)
k_I	Operating current ratio, I_L / I_{nom}
M&V	Measurement and verification
PDI	Pellet durability index
SFT	Swiss Institute of Feed Technology

SEU	Significant Energy Use
η_{global}	Global (electrical-to-useful) efficiency
η_{proc}	Process-stage efficiency
ϕ_i	Loss fraction at stage i
$W_{i,\text{ref}}$	Reference specific energy index (SFT)
W_0	Total resistance coefficient (bulk solids transport)

References

1. Lancheros, J.P.; Espinosa, C.D.; Stein, H.H. Effects of Particle Size Reduction, Pelleting, and Thermal Processing on Digestibility of Energy and Nutrients in Diets Fed to Pigs. *Anim. Feed Sci. Technol.* **2020**, *268*, 114597. [CrossRef]
2. Lyu, F.; Thomas, M.; Hendriks, W.H.; van der Poel, A.F.B. Size Reduction in Feed Technology and Methods for Determining, Expressing and Predicting Particle Size: A Review. *Anim. Feed Sci. Technol.* **2020**, *261*, 114347. [CrossRef]
3. Crespo Sánchez, G.; Monteagudo Yanes, J.P.; Montesino Pérez, M.; Cabrera Sánchez, J.L.; Padrón Padrón, A.; Haeseldonckx, D. Efficiency in Electromechanical Drive Motors and Energy Performance Indicators for Implementing a Management System in Balanced Animal Feed Manufacturing. *Energy* **2020**, *194*, 116818. [CrossRef]
4. Wondra, K.J.; Hancock, J.D.; Behnke, K.C.; Hines, R.H.; Stark, C.R. Effects of Particle Size and Pelleting on Growth Performance, Nutrient Digestibility, and Stomach Morphology in Finishing Pigs. *J. Anim. Sci.* **1995**, *73*, 757–763. [CrossRef] [PubMed]
5. Rojas, O.J.; Stein, H.H. Processing of Ingredients and Diets and Effects on Nutritional Value for Pigs. *J. Anim. Sci. Biotechnol.* **2017**, *8*, 48. [CrossRef] [PubMed]
6. De Jong, J.A.; DeRouchey, J.M.; Tokach, M.D.; Goodband, R.D.; Nelssen, J.L.; Dritz, S.S. Effects of corn particle size, complete diet grinding, and diet form on finishing pig growth performance, caloric efficiency, carcass characteristics, and economics. *Kans. Agric. Exp. Stn. Res. Rep.* **2012**, *10*, 316–324. [CrossRef]
7. Hancock, J.D.; Behnke, K.C. Use of Ingredient and Diet Processing Technologies to Produce Quality Feeds for Pigs. In *Swine Nutrition*; CRC Press: Boca Raton, FL, USA, 2001; pp. 469–497.
8. Abdollahi, M.R.; Zaefarian, F.; Ravindran, V. Feed Intake Response of Broilers: Impact of Feed Processing. *Sci. Rep.* **2023**, *13*, 11282. [CrossRef]
9. Castillo Alvarez, Y.; Jiménez Borges, R.; Monteagudo Yanes, J.P.; Rodríguez Pérez, B.; Patiño Vidal, C.D.; Pfuyo Muñoz, R. Mathematical Model to Improve Energy Efficiency in Hammer Mills and Its Use in the Feed Industry: Analysis and Validation in a Case Study in Cuba. *Processes* **2025**, *13*, 1523. [CrossRef]
10. Bitra, V.S.P.; Womac, A.R.; Chevanan, N.; Miu, P.I.; Igathinathane, C.; Sokhansanj, S.; Smith, D.R. Direct Mechanical Energy Measures of Hammer Mill Comminution of Switchgrass, Wheat Straw, and Corn Stover and Analysis of Their Particle Size Distributions. *Powder Technol.* **2009**, *193*, 32–45. [CrossRef]
11. Bitra, V.S.P.; Womac, A.R.; Igathinathane, C.; Miu, P.I.; Yang, Y.T.; Smith, D.R.; Chevanan, N.; Sokhansanj, S. Direct Measures of Mechanical Energy for Knife Mill Size Reduction of Switchgrass, Wheat Straw, and Corn Stover. *Bioresour. Technol.* **2009**, *100*, 6578–6585. [CrossRef] [PubMed]
12. Mani, S.; Tabil, L.G.; Sokhansanj, S. Grinding Performance and Physical Properties of Wheat and Barley Straws, Corn Stover and Switchgrass. *Biomass Bioenergy* **2004**, *27*, 339–352. [CrossRef]
13. Ghorbani, Z.; Masoumi, A.A.; Hemmat, A. Specific Energy Consumption for Reducing the Size of Alfalfa Chops Using a Hammer Mill. *Biosyst. Eng.* **2010**, *105*, 34–40. [CrossRef]
14. Tumuluru, J.S.; Tabil, L.G.; Song, Y.; Iroba, K.L.; Meda, V. Grinding Energy and Physical Properties of Chopped and Hammer-Milled Barley, Wheat, Oat, and Canola Straws. *Biomass Bioenergy* **2014**, *60*, 58–67. [CrossRef]
15. Naimi, L.J.; Collard, F.; Bi, X.; Lim, C.J.; Sokhansanj, S. Development of Size Reduction Equations for Calculating Power Input for Grinding Pine Wood Chips Using Hammer Mill. *Biomass Convers. Biorefin.* **2016**, *6*, 397–405. [CrossRef]
16. Miao, Z.; Grift, T.E.; Hansen, A.C.; Ting, K.C. Energy Requirement for Comminution of Biomass in Relation to Particle Physical Properties. *Ind. Crops Prod.* **2011**, *33*, 504–513. [CrossRef]
17. Arthur, J.F.; Kepner, R.A.; Dobie, J.B.; Miller, G.E.; Parsons, P.S. Tub Grinder Performance with Crop and Forest Residues. *Trans. ASAE* **1982**, *25*, 1488–1494. [CrossRef]
18. Pradhan, P.; Mahajani, S.M.; Arora, A. Production and Utilization of Fuel Pellets from Biomass: A Review. *Fuel Process. Technol.* **2018**, *181*, 215–232. [CrossRef]
19. Vukmirović, Đ.; Čolović, R.; Rakita, S.; Bržek, T.; Đuragić, O.; Pezo, L. Importance of the Grinding Process and Particle Size in Feed Technology. *Anim. Feed Sci. Technol.* **2017**, *233*, 133–144. [CrossRef]
20. Fang, Q.; Bölöni, I.; Haque, E.; Spillman, C.K. Comparison of Energy Efficiency Between a Roller Mill and a Hammer Mill. *Appl. Eng. Agric.* **1997**, *13*, 631–635. [CrossRef]

21. Svihus, B.; Kløvstad, K.H.; Perez, V.; Zimonja, O.; Sahlström, S.; Schuller, R.B.; Jeksrud, W.K.; Prestløkken, E. Physical and Nutritional Effects of Pelleting of Broiler Chicken Diets Made from Wheat Ground to Different Coarseness by the Use of Roller Mill and Hammer Mill. *Anim. Feed Sci. Technol.* **2004**, *117*, 281–293. [CrossRef]
22. Martin, S.; Behnke, K.C. Grinding: A Review of Hammermill and Roller Mill Performance. *Feed Manag.* **1981**, *32*, 18–24.
23. Mugabi, R.; Byaruhanga, Y.B.; Eskridge, K.M.; Weller, C.L. Effect of Hammer Mill Screen Size and Grain Moisture Content on Milling Energy and Particle Size. *J. Food Res.* **2017**, *6*, 35–46. [CrossRef]
24. Muntean, I.; Rus, F.; Ros, V. Aspects Regarding the Energy Consumption at the Grinding of Fodder Cereals with Hammer Mills. *Bull. Transilv. Univ. BraŞov Ser. II* **2013**, *6*, 69–74.
25. Temmerman, M.; Jensen, P.D.; Hebert, J. Von Rittinger theory adapted to wood chip and pellet milling, in a laboratory scale hammermill. *Biomass Bioenergy* **2013**, *56*, 70–81. [CrossRef]
26. Thomas, M.; van Zuilichem, D.J.; van der Poel, A.F.B. Physical Quality of Pelleted Animal Feed. 2. Contribution of Processes and Its Conditions. *Anim. Feed Sci. Technol.* **1997**, *64*, 173–192. [CrossRef]
27. Abdollahi, M.R.; Ravindran, V.; Svihus, B. Pelleting of Broiler Diets: An Overview with Emphasis on Pellet Quality and Nutritional Value. *Anim. Feed Sci. Technol.* **2013**, *179*, 1–23. [CrossRef]
28. *ASAE S319.4*; Method of Determining and Expressing Fineness of Feed Materials by Sieving, Technical Report. American Society of Agricultural and Biological Engineers: St. Joseph, MI, USA, 2008.
29. Wang, X.; Tian, H.; Xiao, Z.; Zhao, K.; Li, D.; Wang, D. Numerical Simulation and Experimental Study of Corn Straw Grinding Process Based on Computational Fluid Dynamics–Discrete Element Method. *Agriculture* **2024**, *14*, 325. [CrossRef]
30. Pezo, L.; Jovanović, A.; Pezo, M.; Ćurčić, B.L.; Nedeljković, N. Modified Screw Conveyor–Mixers: Discrete Element Modeling Approach. *Adv. Powder Technol.* **2018**, *29*, 1484–1493. [CrossRef]
31. Fernández, J.W.; Cleary, P.W.; McBride, W. Effect of Screw Design on Hopper Draw Down of Spherical Particles in a Horizontal Screw Feeder. *Chem. Eng. Sci.* **2011**, *66*, 5585–5601. [CrossRef]
32. Minglani, D.; Sharma, A.; Pandey, H.; Dayal, R.; Joshi, J.B.; Subramaniam, S. A Review of Granular Flow in Screw Feeders and Conveyors. *Powder Technol.* **2020**, *366*, 369–381. [CrossRef]
33. Pezo, M.; Pezo, L.; Lončar, B.; Kojić, P.; Ilić, M.; Jovanović, A. Granular Flow in Screw Conveyors: A Review of Experiments and Discrete Element Method (DEM) Studies. *Powder Technol.* **2025**, *459*, 121040. [CrossRef]
34. Tian, Y.; Yuan, P.; Yang, F.; Gu, J.; Chen, M.; Tang, J.; Su, Y.; Ding, T.; Zhang, K.; Cheng, Q. Research on the Principle of a New Flexible Screw Conveyor and Its Power Consumption. *Appl. Sci.* **2018**, *8*, 1038. [CrossRef]
35. Wulantuya; Zhang, X.; Hu, Z. Optimization of Operating Parameters of a Screw Conveyor by the Discrete Element Method. *IOP Conf. Ser. Mater. Sci. Eng.* **2020**, *892*, 012073. [CrossRef]
36. Karwat, B.; Rubacha, P.; Stańczyk, E. Optimization of a Screw Conveyor's Exploitation Parameters. *Eksploat. I Niezawodn.—Maint. Reliab.* **2021**, *23*, 285–293. [CrossRef]
37. Bortolamasi, M.; Fottner, J. Design and Sizing of Screw Feeders. In Proceedings of the Partec International Congress for Particle Technology, Nuremberg, Germany, 27–29 March 2001.
38. Kalay, E.; Boğoçlu, M.E.; Bolat, B. Mass Flow Rate Prediction of Screw Conveyor Using Artificial Neural Network Method. *Powder Technol.* **2022**, *408*, 117757. [CrossRef]
39. Dehghani-Sanij, A.R.; Al-Haq, A.; Bastian, J.; Luehr, G.; Nathwani, J.; Fraser, R.A.; Dusseault, M.B. Assessment of Energy-Efficient Electric Motors and Drives in Industrial Applications. *Energy Effic.* **2016**, *9*, 1259–1279.
40. Saidur, R.; Mekhilef, S.; Ali, M.B.; Safari, A.; Mohammed, H.A. Applications of Variable Speed Drive (VSD) in Electrical Motors Energy Savings. *Renew. Sustain. Energy Rev.* **2012**, *16*, 543–550. [CrossRef]
41. Fuchs, H.; Aghajanzadeh, A.; Therkelsen, P. Identification of Drivers, Benefits and Challenges of ISO 50001 through Case Study Content Analysis. *Energy Policy* **2020**, *142*, 111443. [CrossRef]
42. Marimon, F.; Casadesús, M. Reasons to Adopt ISO 50001 Energy Management System. *Sustainability* **2017**, *9*, 1740. [CrossRef]
43. Fitzgerald, P.; Therkelsen, P.; Sheaffer, P.; Rao, P. Deeper and Persistent Energy Savings and Carbon Dioxide Reductions Achieved through ISO 50001 in the Manufacturing Sector. *Sustain. Energy Technol. Assess.* **2023**, *57*, 103280. [CrossRef]
44. Kouaho, E.S.; N'Guessan, Y.; Marvillet, C. Comparative Study of an Energy Information System and Energy Management System According to ISO 50001. *Energies* **2024**, *17*, 5446. [CrossRef]
45. *ISO 50015:2014*; Energy Management Systems—Measurement and Verification of Energy Performance of Organizations—General Principles and Guidance, Technical Report. International Organization for Standardization: Geneva, Switzerland, 2014.
46. *ISO 50002-3:2025*; Energy Audits—Part 3: Guidance for Conducting an Energy Audit Using ISO 50002-1 in Processes, Technical Report. International Organization for Standardization: Geneva, Switzerland, 2025.
47. Castillo-Alvarez, Y.; Jiménez-Borges, R.; Alfonso-Francia, G.; Rodríguez-Pérez, B.; Patiño-Vidal, C.D.; Iturralde-Carrera, L.A.; Rodríguez-Reséndiz, J. Transition to a Circular Bioeconomy in the Sugar Agro-Industry: Predictive Modeling to Estimate the Energy Potential of By-Products. *Technologies* **2025**, *13*, 238. [CrossRef]

48. Olivares Ramírez, J.M. Evaluación de la Eficiencia Energética en el Proceso de Molienda de una Fábrica de Piensos y Metodología de Referencia del Swiss Institute of Feed Technology. Master's Thesis, Universidad de Cienfuegos "Carlos Rafael Rodríguez", Cienfuegos, Cuba, 2014.
49. *ISO 50001:2018*; Energy Management Systems—Requirements with Guidance for Use, Technical Report. International Organization for Standardization: Geneva, Switzerland, 2018.
50. *ISO 50001:2018/Amd 1:2024*; Energy Management Systems—Requirements with Guidance for Use—Amendment 1: Climate Action Changes, Technical Report. International Organization for Standardization: Geneva, Switzerland, 2024.
51. *ISO 50006:2023*; Energy Management Systems—Evaluating Energy Performance Using Energy Performance Indicators and Energy Baselines, Technical Report. International Organization for Standardization: Geneva, Switzerland, 2023.
52. *ISO 50004:2020*; Energy Management Systems—Guidance for the Implementation, Maintenance and Improvement of an ISO 50001 Energy Management System, Technical Report. International Organization for Standardization: Geneva, Switzerland, 2020.
53. Schulze, M.; Nehler, H.; Ottosson, M.; Thollander, P. Energy Management in Industry—A Systematic Review of Previous Findings and an Integrative Conceptual Framework. *J. Clean. Prod.* **2016**, *112*, 3692–3708. [CrossRef]
54. Abdelaziz, E.A.; Saidur, R.; Mekhilef, S. A Review on Energy Saving Strategies in Industrial Sector. *Renew. Sustain. Energy Rev.* **2011**, *15*, 150–168. [CrossRef]
55. Hasanbeigi, A.; Price, L. A Review of Energy Use and Energy Efficiency Technologies for the Textile Industry. *Renew. Sustain. Energy Rev.* **2012**, *16*, 3648–3665. [CrossRef]
56. *NEMA MG 1-2021*; Motors and Generators, Technical Report. National Electrical Manufacturers Association: Rosslyn, VA, USA, 2021.
57. *IEC 60034-30-1:2014*; Rotating Electrical Machines—Part 30-1: Efficiency Classes of Line Operated AC Motors (IE Code), Technical Report. International Electrotechnical Commission: Geneva, Switzerland, 2014.
58. Spivakovsky, A.; Dyachkov, V. *Conveying Machines*; Mir Publishers: Moscow, Russia, 1985.
59. Saidur, R. A Review on Electrical Motors Energy Use and Energy Savings. *Renew. Sustain. Energy Rev.* **2010**, *14*, 877–898. [CrossRef]
60. Thirugnanasambandam, M.; Hasanuzzaman, M.; Saidur, R.; Ali, M.B.; Rajakarunakaran, S.; Devaraj, D.; Rahim, N.A. Analysis of Electrical Motors Load Factors and Energy Savings in an Indian Cement Industry. *Energy* **2011**, *36*, 4307–4314. [CrossRef]
61. Waide, P.; Brunner, C.U. *Energy-Efficiency Policy Opportunities for Electric Motor-Driven Systems*; Technical Report; International Energy Agency (IEA): Paris, France, 2011.
62. Magdalinović, N. A Procedure for Rapid Determination of the Bond Work Index. *Int. J. Miner. Process.* **1989**, *27*, 125–132. [CrossRef]
63. von Rittinger, P.R. *Lehrbuch der Aufbereitungskunde*; Ernst & Korn: Berlin, Germany, 1867.
64. Kick, F. *Das Gesetz der Proportionalen Widerstände und Seine Anwendung*; Arthur Felix: Leipzig, Germany, 1885.
65. Walker, W.H.; Lewis, W.K.; McAdams, W.H.; Gilliland, E.R. *Principles of Chemical Engineering*; McGraw-Hill: New York, NY, USA, 1937.
66. Green, D.W.; Perry, R.H. *Perry's Chemical Engineers' Handbook*, 8th ed.; McGraw-Hill: New York, NY, USA, 2008.
67. CEMA. *Bulk Material Handling by Conveyor Belt*; Technical Report; Conveyor Equipment Manufacturers Association: Naples, FL, USA, 2015.
68. *FEM 2.581/2.582*; Bucket Elevators—Rules for the Design of Bucket Elevators, Technical Report. Fédération Européenne de la Manutention: Bruxelles, Belgique, 2000.
69. Woodcock, C.R.; Mason, J.S. *Bulk Solids Handling: An Introduction to the Practice and Technology*; Leonard Hill: Glasgow, UK, 1987.
70. Roberts, A.W. The Influence of Granular Vortex Motion on the Volumetric Performance of Enclosed Screw Conveyors. *Powder Technol.* **1999**, *104*, 56–67. [CrossRef]
71. Owen, P.J.; Cleary, P.W. Prediction of Screw Conveyor Performance Using the Discrete Element Method (DEM). *Powder Technol.* **2009**, *193*, 274–288. [CrossRef]
72. Owen, P.J.; Cleary, P.W. Screw Conveyor Performance: Comparison of Discrete Element Modelling with Laboratory Experiments. *Prog. Comput. Fluid Dyn.* **2010**, *10*, 327–333. [CrossRef]
73. Shimizu, Y.; Cundall, P.A. Three-Dimensional DEM Simulations of Bulk Handling by Screw Conveyors. *J. Eng. Mech.* **2001**, *127*, 864–872. [CrossRef]
74. *FEM 2.121/2.122*; Screw Conveyors for Bulk Materials—Design Rules for Drive Power, Technical Report. Fédération Européenne de la Manutention: Bruxelles, Belgique, 2024.
75. Sakthivel, V.P.; Vasan, P.; Kathirvelan, C. Energy Consumption Pattern in Manufacturing of Different Types of Broiler Feeds. *Indian J. Anim. Nutr.* **2020**, *37*, 366–373. [CrossRef]
76. Gil, M.; Arauzo, I. Hammer Mill Operating and Biomass Physical Conditions Effects on Particle Size Distribution of Solid Pulverized Biofuels. *Fuel Process. Technol.* **2014**, *127*, 80–87. [CrossRef]

77. Islam, M.N.; McRae, K.B. Energy Requirement and Particle Size Distribution in Grinding of Grains. *Can. Agric. Eng.* **1988**, *30*, 241–245.
78. Mei, L.; Xue, S.; Zhang, X. Optimal Design and Experiment of Screw Conveyor Capacity and Power Consumption. *PLoS ONE* **2022**, *17*, e0266948. [CrossRef] [PubMed]
79. Dziki, D. The Crushing of Wheat Kernels and Its Consequence on the Grinding Process. *Powder Technol.* **2008**, *185*, 181–186. [CrossRef]

Disclaimer/Publisher's Note: The statements, opinions and data contained in all publications are solely those of the individual author(s) and contributor(s) and not of MDPI and/or the editor(s). MDPI and/or the editor(s) disclaim responsibility for any injury to people or property resulting from any ideas, methods, instructions or products referred to in the content.